Inorg. Chem. **2007**, *46*, 8871–8886

Electronic Structure of the Sulfonyl and Phosphonyl Groups: A Computational and Crystallographic Study

Emma Denehy, Jonathan M. White, and Spencer J. Williams*

School of Chemistry and Bio21 Molecular Science and Biotechnology Institute, University of Melbourne, Parkville, Victoria, Australia 3010

Received April 11, 2007

A computational and X-ray crystallographic investigation of the electronic and geometric structures of a range of sulfonyl (–SO_2–) and phosphonyl (–PO_2^-–) containing species was undertaken to investigate the nature of valency and bonding in these functional groups. The traditional representation of sulfonyl and phosphonyl species is with octet-violating Lewis structures, which require d-orbital participation at the central atom. However, computational studies cast serious doubt upon this bonding model. In this work, we have employed NBO/NRT analysis to investigate hybridization, atomic formal charges, donor–acceptor interactions, and resonance structure contributions. Our results predict that within sulfonyl and phosphonyl systems, bonding interactions are highly polarized, of the form X^+–Y^- (X = P, S), and possess additional contributions from reciprocal n $\rightarrow$ σ^* interactions where substituents off sulfur or phosphorus simultaneously act as donors and acceptors. Experimental evidence for the proposed bonding arrangement is provided for the sulfonyl functional group through a series of low-temperature X-ray structure correlations for sulfate monoesters, sulfamates, and methanesulfonates. Examination of changes to bond lengths and geometries upon substituent variation support the computational results. Together, our studies lend support for a bonding network in sulfonyl and phosphonyl groups composed of polar interactions augmented with reciprocal hyperconjugative bonding, which does not necessitate significant d-orbital participation nor formal octet violation at the central sulfur or phosphorus.

Introduction

The phosphonyl (−PO_2^-−) and sulfonyl (−SO_2−) functional groups are an essential component of some of the most important molecular species in Nature.[1] Phosphate esters play a critical structural role in nucleic acids and provide the fundamental energy currency in biological systems. Phosphoryl group (−PO_3^{2-}−) transfer has long been held as the paradigm of intracellular communication.[2] Increasingly, it has emerged that sulfuryl group (−SO_3^-−) transfer processes orchestrate extracellular communication in a manner that parallels the role of phosphoryl group transfer in the intracellular domain. Sulfated biomolecules have been implicated in such diverse roles as cell and tissue differentiation during embryogenesis,[3−5] regulation of hormonal activity,[6,7] leukocyte adhesion during inflammation,[8] interspecies communication,[9] and pathogenesis.[10] The critical importance of sulfuryl and phosphoryl transfer has prompted sustained research efforts to elucidate the fine detail of these group transfer reactions.[11−16] An intimate understanding of the

* To whom correspondence should be addressed. E-mail: sjwill@unimelb.edu.au.

(1) The following terms are used to denote the corresponding groups: phosphoryl, −PO_3^{2-}; sulfuryl, −SO_3−; phosphonyl, −PO_2^-−; sulfonyl, −SO_2−. While the phosphoryl and sulfuryl groups are more correctly referred to as phosphonato and sulfonato, respectively, we have retained the common usage because it is more widespread in the literature.

(2) Westheimer, F. H. *Science* **1987**, *235*, 1173−1178.
(3) Whitelock, J. M.; Iozzo, R. V. *Chem. Rev.* **2005**, *105*, 2745−2764.
(4) Nakato, H.; Kimata, K. *Biochim. Biophys. Acta* **2002**, *1573*, 312−318.
(5) Taylor, K. R.; Gallo, R. L. *FASEB J.* **2006**, *20*, 9−22.
(6) Strott, C. A. *Endocr. Rev.* **2002**, *23*, 703−732.
(7) Reed, M. J.; Purohit, A.; Woo, L. W. L.; Newman, S. P.; Potter, B. V. L. *Endocr. Rev.* **2005**, *26*, 171−202.
(8) Kehoe, J. W.; Bertozzi, C. R. *Chem. Biol.* **2000**, *7*, R57−R61.
(9) Cullimore, J. V.; Ranjeva, R.; Bono, J. J. *Trends Plant Sci.* **2001**, *6*, 24−30.
(10) Mougous, J. D.; Green, R. E.; Williams, S. J.; Brenner, S. E.; Bertozzi, C. R. *Chem. Biol.* **2002**, *9*, 767−776.
(11) Williams, A. *Acc. Chem. Res.* **1989**, *22*, 387−392.
(12) Thatcher, G. R. J.; Kluger, R. *Adv. Phys. Org. Chem.* **1989**, *25*, 99−265.
(13) Cleland, W. W.; Hengge, A. C. *Chem. Rev.* **2006**, *106*, 3252−3278.
(14) Hengge, A. C. *Acc. Chem. Res.* **2002**, *35*, 105−112.
(15) King, J. F.; Skonieczny, S.; Khemani, K. C.; Lock, J. D. *Adv. Chem. Ser.* **1987**, 385−398.

10.1021/ic700687t CCC: $37.00
Published on Web 09/19/2007

ground-state electronic structure of the sulfonyl and phosphonyl functionalities should improve understanding of these transfer reactions.

There remains considerable uncertainty of the fundamental electronic structure of phosphonyl and, particularly, sulfonyl functional groups because of the apparent octet violation of the central phosphorus and sulfur atoms. While many undergraduate chemistry textbooks state that elements in the third period and higher may violate the octet rule through occupation of d-orbitals,[17−19] a significant involvement of d-orbitals in bonding in hypervalent phosphorus and sulfur species seems doubtful. Since the seminal study of Reed and von Rague Schleyer nearly 20 years ago,[20] considerable computational evidence has mounted supporting alternative bonding models in hypervalent sulfur and phosphorus species that do not require d-orbital occupation.[21−26] While inclusion of d-orbitals in basis sets are required for accurate calculation of hypervalent phosphorus and sulfur species, their inclusion serves primarily as polarization functions.[27] The principal objection to the involvement of d-orbitals in bonding in such species is the significant energy required to promote electrons to these orbitals.[28] In addition, d-orbitals are diffuse and orbital overlap with adjacent donor orbitals is expected to be poor; however, it has been argued that in high oxidation states d-orbital contraction occurs allowing better overlap with donor orbitals.[29] Alternative models for bonding in hypervalent oxysulfur and oxyphosphorus species invoke either X^+-Y^- dipolar or 3-center, 4-electron bonding.[28]

While there is a substantial body of computational studies on the nature of bonding in hypervalent phosphorus and sulfur species, there are precious few experimental studies explicitly investigating this topic. Studies of bonding in hypervalent phosphorus and sulfur species, including sulfur diimides and sulfur triimides,[30] phosphine oxides,[31] iminophosphoranes,[32] phosphorus tetrahalides,[33] phosphazenes,[34] and representatives from various sulfur-containing functional groups,[35,36] support highly polarized modes of bonding, rather than bonding models that require d-orbital participation. Consequently, to gain deeper insight into the nature of bonding within the sulfonyl and phosphonyl functional groups, we undertook a combined computational and experimental study on the electronic structure of the sulfonyl and phosphonyl functional groups. As more experimental data has been obtained for phosphonyl systems, we have maintained a particular focus on the corresponding data for sulfonyl systems.

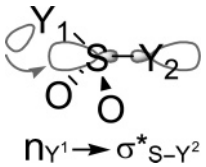

Figure 1. Illustration of generalized $n_{Y^1} \rightarrow \sigma^*_{S-Y^2}$ interaction in sulfonyl systems.

Preliminary experimental insight into the electronic structure of the sulfonyl functionality was provided from our recent study of sulfonyl group transfer, where the ground-state conformations of a large number of sulfate monoesters and sulfamate esters in the solid-state implied operation of an $n_{Y^1} \rightarrow \sigma^*_{S-O}$ ($Y^1 = NH_2, O^-$) hyperconjugative interaction in the equilibrium structures of these compounds.[37] There is good evidence for operation of a generalized $n_{Y^1} \rightarrow \sigma^*_{S-Y^2}$ (Y^1 = electron-donating group, Y^2 = electron-withdrawing group) interaction in the equilibrium structure of sulfonyl systems (Figure 1), which has been investigated using structural methods in the gas, solution, and solid state. X-ray crystallographic studies of numerous sulfonyl systems,[38−44] suggest that an *anti* conformation about the $S-Y^1$ bond is a common architectural feature in these species. This conformation allows for efficient $n_{Y^1} \rightarrow \sigma^*_{S-Y^2}$ orbital overlap. A similar conformational preference is found for sulfonyl systems in the gas phase through electron and microwave diffraction studies[45,46] and in the solution-phase by ^{1}H NMR spectroscopy.[42,47−51] The reactivity of various sulfonyl systems has been rationalized in terms of operation of an $n_{Y^1} \rightarrow \sigma^*_{S-Y^2}$ interaction including the facility of generation of α-sulfonyl carbanions[52] and the increased acidity[53−55] and

(16) Gordon, I. M.; Maskill, H.; Ruasse, M. F. *Chem. Soc. Rev.* **1989**, *18*, 123−151.
(17) Kotz, J. C.; Treichel, P. M.; Weaver, G. C. *Chemistry and Chemical Reactivity*; Thomson Brooks/Cole: Belmont, CA, 2006; p 394.
(18) Brown, T. L.; LeMay, H. E., Jr.; Bursten, B. E. *Chemistry the Central Science*; Pearson Education Inc.: Upper Saddle River, NJ, 2006; p327.
(19) Zumdahl, S. S.; Zumdahl, S. A. *Chemistry*, 6 ed.; Houghton Mifflin Company: Boston, MA, 2003; pp 606−607.
(20) Reed, A. E.; Schleyer, P. V. *J. Am. Chem. Soc.* **1990**, *112*, 1434−1445.
(21) Gillespie, R. J.; Silvi, B. *Coord. Chem. Rev.* **2002**, *233*, 53−62.
(22) Cioslowski, J.; Mixon, S. T. *Inorg. Chem.* **1993**, *32*, 3209−3216.
(23) Dobado, J. A.; Martinez-Garcia, H.; Molina, J. M.; Sundberg, M. R. *J. Am. Chem. Soc.* **1998**, *120*, 8461−8471.
(24) Dobado, J. A.; Martinez-Garcia, H.; Molina, J. M.; Sundberg, M. R. *J. Am. Chem. Soc.* **1999**, *121*, 3156−3164.
(25) Dobado, J. A.; Martinez-Garcia, H.; Molina, J. M.; Sundberg, M. R. *J. Am. Chem. Soc.* **2000**, *122*, 1144−1149.
(26) Suidan, L.; Badenhoop, J. K.; Glendening, E. D.; Weinhold, F. *J. Chem. Educ.* **1995**, *72*, 583−586.
(27) Magnusson, E. *J. Am. Chem. Soc.* **1993**, *115*, 1051−1061.
(28) Huheey, J. E.; Keiter, E. A.; Keiter, R. L. *Inorganic Chemistry: Principles of Structure and Reactivity*, 4th ed.; Harper Collins College Publishers: New York, 1993; pp 866−876.
(29) Mitchell, K. A. R. *Chem. Rev.* **1969**, *69*, 157−178.
(30) Leusser, D.; Henn, J.; Kocher, N.; Engels, B.; Stalke, D. *J. Am. Chem. Soc.* **2004**, *126*, 1781−1793.
(31) Chesnut, D. B. *J. Am. Chem. Soc.* **1998**, *120*, 10504−10510.
(32) Kocher, N.; Leusser, D.; Murso, A.; Stalke, D. *Chem.—Eur. J.* **2004**, *10*, 3622−3631.
(33) Heil, T. E.; Check, C. E.; Lobring, K. C.; Sunderlin, L. S. *J. Phys. Chem. A* **2002**, *106*, 10043−10048.
(34) Chaplin, A. B.; Harrison, J. A.; Dyson, P. J. *Inorg. Chem.* **2005**, *44*, 8407−8417.
(35) Chesnut, D. B.; Quin, L. D. *Heteroat. Chem.* **2004**, *15*, 216−224.
(36) Gassman, P. G.; Callstrom, M. R.; Martin, J. C.; Rongione, J. C. *J. Am. Chem. Soc.* **1988**, *110*, 8724−8725.
(37) Denehy, E.; White, J. M.; Williams, S. J. *Chem. Commun.* **2006**, 314−316.
(38) King, J. F.; Khemani, K. C.; Skonieczny, S.; Payne, N. C. *Chem. Commun.* **1988**, 415−417.
(39) Belvisi, L.; Carugo, O.; Poli, G. *J. Mol. Struct.* **1994**, *318*, 189−202.
(40) Oppolzer, W.; Chapuis, C.; Bernardinelli, G. *Tetrahedron Lett.* **1984**, *25*, 5885−5888.
(41) Barrett, A. G. M.; Braddock, D. C.; Christian, P. W. N.; Pilipauskas, D.; White, A. J. P.; Williams, D. J. *J. Org. Chem.* **1998**, *63*, 5818−5823.
(42) Lyapkalo, I. M.; Reissig, H. U.; Schafer, A.; Wagner, A. *Helv. Chim. Acta* **2002**, *85*, 4206−4215.
(43) Gais, H. J.; Vollhardt, J.; Lindner, H. J. *Angew. Chem., Int. Ed. Engl.* **1986**, *25*, 939−941.
(44) Raabe, G.; Gais, H. J.; Fleischhauer, J. *J. Am. Chem. Soc.* **1996**, *118*, 4622−4630.

susceptibility to nucleophilic attack at sulfur[38] of cyclic sulfonyl systems relative to their acyclic counterparts.

The presence of an $n_{Y^1} \rightarrow \sigma^*_{S-Y^2}$ ($Y^1 = CH_3$, CH_2^-, NH_2; $Y^2 =$ C, O, halogen) interaction in sulfonyl systems has also been the subject of some theoretical attention.[20,44,56−61] However, in all of these studies but one,[20] the $n_{Y^1} \rightarrow \sigma^*_{S-Y^2}$ interaction was studied in isolation, without considering that this interaction may compose part of a highly delocalized bonding network within the sulfonyl functional group. Surprisingly, the n_Y-donor ability of the sulfonyl oxygens has been ignored, despite the fact that in most of the systems subject to computational scrutiny the sulfonyl oxygens are the most potent n_Y-donors. Furthermore, the *reciprocity* of these interactions, that is, where the sulfonyl substituents can act simultaneously as hyperconjugative donors and acceptors, has, by and large, been ignored.

The electronic structure of oxyphosphorus species has received significantly more attention than that of oxysulfur species.[62] There is considerable interest in the role of hyperconjugation in oxyphosphorus species. An $n_{Y^1} \rightarrow \sigma^*_{P-Y^2}$ ($Y^1 =$ O, CR_2^-; $Y^2 =$ H, F, Cl, CH_3, Ph) interaction was proposed to account for bonding in phosphine oxides and phosphonium ylides.[62] Denmark and co-workers proposed operation of hyperconjugative interactions in phosphorus-stabilized carbanions through a combination of theoretical and experimental methods,[63,64] while Cramer and co-workers have proposed that hyperconjugation plays a major role in determination of the constitutional isomerism displayed by five-coordinate, trigonal-bipyramidal phosphorus species.[65,66] Wilke and Weinhold recently proposed that the electronic structure of phosphodioxirane was consistent with a 3-center, 4-electron, Pimentel−Rundle bonding scheme.[67] Furthermore, Ruben and co-workers have suggested a generalized anomeric effect is responsible for P−N bond lability in phosphagens.[68]

Here, we present the results of calculations on the electronic structure of sulfonyl and phosphonyl groups employing natural bond orbital (NBO) analysis. The results of these calculations suggest a highly similar bonding arrangement in these functional groups involving not only a highly polarized interaction between the central phosphorus or sulfur and its substituents but also possessing important contributions from reciprocal $n_{Y^1} \rightarrow \sigma^*_{S-Y^2}$ or $n_{Y^1} \rightarrow \sigma^*_{P-Y^2}$ hyperconjugative interactions. The reciprocal nature of these hyperconjugative elements suggests operation of a highly delocalized bonding network, reminiscent of 5-center, 8-electron bonding. The effect of substituent variation on these delocalization interactions in the sulfonyl and phosphonyl systems has been investigated using NBO analysis.

This work also aims to redress the lack of experimental studies on bonding in hypervalent sulfur species. Three structure−reactivity correlations have been constructed using low-temperature X-ray structural data for sulfate monoesters, sulfamate esters, and methanesulfonate (mesylate) esters. These data allow comparison of experimentally and computationally determined effects of substituent variation within the sulfonyl functional group. Alteration of substituent donor−acceptor ability within these sulfonyl systems results in changes in key geometric parameters in the X-ray crystallographic data consistent with the conclusions drawn from NBO analysis.

Experimental Methods

All calculations were performed using the GAUSSIAN 03 package.[69] Unless specified, geometric parameters and energies are presented at the mPW1PW91/6-311++G(3df,2p) level of theory. The natures of stationary points were confirmed by performing frequency calculations on the optimized structures. Population analyses were performed using the NBO 5.0[70] module as implemented in GAUSSIAN 03 at the RHF/6-311++G(3df,2p) level of theory. NRT analysis was performed as implemented in the NBO

(45) Hargittai, I. *The Structure of Volatile Sulfur Compounds*; Kluwer Academic Publishers: Dordrecht, The Netherlands, 1985; 316 pp.
(46) Hargittai, I. Structural chemistry of gaseous sulfoxides and sulfones. In *The Chemistry of Sulphones and Sulphoxides*; Patai, S., Rappoport, Z., Stirling, C. J. M., Eds.; Wiley: Chichester, U.K., 1988; pp 33−53.
(47) Jennings, W. B.; Spratt, R. *J. Chem. Soc. D* **1970**, 1418−1419.
(48) Gais, H. J.; Hellmann, G.; Gunther, H.; Lopez, F.; Lindner, H. J.; Braun, S. *Angew. Chem., Int. Ed. Engl.* **1989**, *28*, 1025−1028.
(49) Gais, H. J.; Hellmann, G.; Lindner, H. J. *Angew. Chem., Int. Ed. Engl.* **1990**, *29*, 100−103.
(50) Gais, H. J.; Hellmann, G. *J. Am. Chem. Soc.* **1992**, *114*, 4439−4440.
(51) Laughlin, R. G. *J. Am. Chem. Soc.* **1967**, *89*, 4268−4271.
(52) Boche, G. *Angew. Chem., Int. Ed.* **1989**, *28*, 277−297.
(53) Andersen, K. K.; Kociolek, M. G. *J. Org. Chem.* **1995**, *60*, 2003−2007.
(54) Girard, Y.; Atkinson, J. G.; Rokach, J. *J. Chem. Soc., Perkin Trans. 1* **1979**, 1043−1047.
(55) Burke, P. O.; McDermott, S. D.; Hannigan, T. J.; Spillane, W. J. *J. Chem. Soc., Perkin Trans. 2* **1984**, 1851−1854.
(56) Wolfe, S.; Stolow, A.; Lajohn, L. A. *Tetrahedron Lett.* **1983**, *24*, 4071−4074.
(57) Gais, H. J.; Lenz, D.; Raabe, G. *Tetrahedron Lett.* **1995**, *36*, 7437−7440.
(58) Henderson, K. W.; Kennedy, A. R.; MacDougall, D. J.; Shanks, D. *Organometallics* **2002**, *21*, 606−616.
(59) Bharatam, P. V.; Amita; Senthilkumar, P. *Tetrahedron* **2004**, *60*, 4801−4805.
(60) Bharatam, P. V.; Kaur, A.; Kaur, D. *Tetrahedron* **2002**, *58*, 10335−10339.
(61) Bharatam, P. V.; Amita, A. G.; Kaur, D. *Tetrahedron* **2002**, *58*, 1759−1764.
(62) Gilheany, D. G. *Chem. Rev.* **1994**, *94*, 1339−1374.
(63) Denmark, S. E.; Cramer, C. J. *J. Org. Chem.* **1990**, *55*, 1806−1813.
(64) Cramer, C. J.; Denmark, S. E.; Miller, P. C.; Dorow, R. L.; Swiss, K. A.; Wilson, S. R. *J. Am. Chem. Soc.* **1994**, *116*, 2437−2447.
(65) Cramer, C. J.; Gustafson, S. M. *J. Am. Chem. Soc.* **1993**, *115*, 9315−9316.
(66) Cramer, C. J. *J. Mol. Struct.* (*THEOCHEM*) **1996**, *370*, 135−146.
(67) Wilke, J. J.; Weinhold, F. *J. Am. Chem. Soc.* **2006**, *128*, 11850−11859.
(68) Ruben, E. A.; Chapman, M. S.; Evanseck, J. D. *J. Am. Chem. Soc.* **2005**, *127*, 17789−17798.
(69) Frisch, M. J.; Trucks, G. W.; Schlegel, H. B.; Scuseria, G. E.; Robb, M. A.; Cheeseman, J. R.; Montgomery, J. A., Jr.; Vreven, T.; Kudin, K. N.; Burant, J. C.; Millam, J. M.; Iyengar, S. S.; Tomasi, J.; Barone, V.; Mennucci, B.; Cossi, M.; Scalmani, G.; Rega, N.; Petersson, G. A.; Nakatsuji, H.; Hada, M.; Ehara, M.; Toyota, K.; Fukuda, R.; Hasegawa, J.; Ishida, M.; Nakajima, T.; Honda, Y.; Kitao, O.; Nakai, H.; Klene, M.; Li, X.; Knox, J. E.; Hratchian, H. P.; Cross, J. B.; Bakken, V.; Adamo, C.; Jaramillo, J.; Gomperts, R.; Stratmann, R. E.; Yazyev, O.; Austin, A. J.; Cammi, R.; Pomelli, C.; Ochterski, J. W.; Ayala, P. Y.; Morokuma, K.; Voth, G. A.; Salvador, P.; Dannenberg, J. J.; Zakrzewski, V. G.; Dapprich, S.; Daniels, A. D.; Strain, M. C.; Farkas, O.; Malick, D. K.; Rabuck, A. D.; Raghavachari, K.; Foresman, J. B.; Ortiz, J. V.; Cui, Q.; Baboul, A. G.; Clifford, S.; Cioslowski, J.; Stefanov, B. B.; Liu, G.; Liashenko, A.; Piskorz, P.; Komaromi, I.; Martin, R. L.; Fox, D. J.; Keith, T.; Al-Laham, M. A.; Peng, C. Y.; Nanayakkara, A.; Challacombe, M.; Gill, P. M. W.; Johnson, B.; Chen, W.; Wong, M. W.; Gonzalez, C.; Pople, J. A. *Gaussian 03*, revision B.04; Gaussian, Inc.: Pittsburgh, PA, 2003.

5.0 module.[71−73] The default NRT search was used and employed the full-density matrix option for NRT optimization using the "NRTFDM" keyword because of the possible formal hypervalency of the central phosphorus or sulfur atom. Optimized geometries of all species investigated computationally are listed in the Supporting Information.

For the structure−reactivity correlations, all compounds were synthesized according to standard literature procedures.[74−79] Intensity data were collected with a Bruker SMART Apex CCD detector using Mo Kα radiation (graphite crystal monochromator λ = 0.71073). Data were reduced using the program SAINT.[80] The temperature during data collection was maintained at 130.0(2) K using an Oxford Cryostream cooling device. The structures were solved by direct methods and difference Fourier synthesis. Thermal ellipsoid plots were generated using the program ORTEP-3[81] integrated within the WINGX[82] suite of programs.

For crystallographic data for the sulfonate ester series, see Supporting Information. Experimental details and crystallization data for the sulfate monoester and sulfamate ester series have been reported previously.[37]

Results and Discussion

Benchmarking of Computational Methods. It has been reported that for the modeling of hypervalent sulfur species, larger split-valence basis sets are required for adequate agreement with experimental data; best agreement occurs through incorporation of an f (polarization) function on sulfur.[83−85] Accordingly, calculations have been performed using a 6-311++G(3df,2p) basis set. Diffuse functions have been employed because of the presence of multiple lone pairs and the formal negative charge on many of the species under investigation. The mPW1PW91 hybrid density functional theory has been employed because of its reported superiority in predicting accurate geometries for oxysulfur species. Specifically, in a series of calculations employing various ab initio and DFT electron correlation methods, including MP2, QCISD(T), and various density functional methods, Typke and Dakkouri found best agreement with their electron diffraction structure of dimethyl sulfoxide when the PW91 correlation functional was employed in their geometry optimizations.[86] Comparison between experimentally determined X-ray crystal structures (vide infra) and calculated values reveal good to excellent agreement between theory and experiment. Comparison of the sulfonyl nonbridging bond lengths for each of the calculated species $MeOSO_2Y^1$ (Y^1 = CH_3, NH_2, O^-) with the X-ray crystal data for the corresponding compounds with the highest parent phenol pK_a value (4-nitrobenzyl mesylate, ethyl sulfamate, and potassium methyl sulfate) reveals excellent agreement between experiment and theory (<0.0035 Å). For the S−Y^1 bond, there is also good agreement between the experimental and calculated values, respectively (r_{S-C} = 1.7591(14) vs 1.7564 Å; r_{S-N} = 1.5975(14) vs 1.6159 Å; $r_{S-O(anti)}$ = 1.4411(19) vs 1.4403 Å). There is weaker agreement between experimentally determined and calculated S−O bridging bond distances; however, the differences are relatively small ($r_{S-O(mesylate)}$ = 1.5782(10) vs 1.5887 Å; $r_{S-O(sulfamate)}$ = 1.5694(11) vs 1.5815 Å; $r_{S-O(sulfate)}$ = 1.6019(19) vs 1.6509 Å). The poorer agreement between the calculated and experimental values for the sulfur-bridging oxygen bond may be ascribed to environmental effects, especially structural changes resulting from electronic rearrangement to promote charge stabilization. Decreased charge stability in the gas-phase relative to the solid state should result in increased donation into the S−O_{bridge} antibonding orbital, resulting in a longer S−O_{bridge} bond; this argument is supported by the increasing discrepancy between experiment and theory with increasing Y^1-donor ability.

Table 1. Comparison of Predicted and Experimental Bond Lengths for Sulfur Trioxide (SO_3)

	exptl	B3LYP/ 6-311++G(3df,2p)	mPW1PW91/ 6-311++G(3df,2p)
S−O bond length (Å)	1.4198	1.4253	1.417
difference ($\times 10^{-3}$ Å)		5.5	2.8

Geometry optimizations performed using the B3LYP hybrid functional predict longer bond lengths than by other methods; indeed, the bond lengths of sulfur trioxide were overestimated using B3LYP, while the use of mPW1PW91 provided more acceptable agreement with the experimentally determined value (Table 1).[87] Lill and co-workers have reported that geometries optimized using B3LYP tend to provide higher estimates of $E(2)$ values relative to geometries optimized using different density functional methods,[88] indicating either a relative overestimation of the donor orbital energy or, more likely, an underestimation of the acceptor orbital energy. These data indicate that caution should be exercised with the use of B3LYP in geometry calculations of species where σ^*-orbital occupancy is expected to contribute significantly to bonding, such as those under investigation here.

(70) Glendening, E. D.; Badenhoop, J. K.; Reed, A. E.; Carpenter, J. E.; Bohmann, C. M.; Morales, C. M.; Weinhold, F. *NBO 5.0*; Theoretical Chemistry Institute, University of Wisconsin: Madison, WI, 2001.
(71) Glendening, E. D.; Weinhold, F. *J. Comput. Chem.* **1998**, *19*, 593−609.
(72) Glendening, E. D.; Weinhold, F. *J. Comput. Chem.* **1998**, *19*, 610−627.
(73) Glendening, E. D.; Badenhoop, J. K.; Weinhold, F. *J. Comput. Chem.* **1998**, *19*, 628−646.
(74) Burkhardt, G. N.; Lapworth, A. *J. Chem. Soc.* **1926**, 684−690.
(75) Lloyd, A. G.; Dodgson, K. S.; Tudball, N. *Biochim. Biophys. Acta* **1961**, *52*, 413−419.
(76) Appel, R.; Berger, G. *Chem. Ber.* **1958**, *91*, 1339−1341.
(77) Okada, M.; Iwashita, S.; Koizumi, N. *Tetrahedron Lett.* **2000**, *41*, 7047−7051.
(78) Yamada, K.; Kurokawa, T.; Tokuyama, H.; Fukuyama, T. *J. Am. Chem. Soc.* **2003**, *125*, 6630−6631.
(79) Lo, Y. S.; Nolan, J. C.; Shamblee, D. A., Sulfamates as antiglaucoma agents. U.S. Patent 5,192,785, 1993.
(80) *SMART, SAINT, SADABS*; Siemens Analytical X-ray Instruments, Inc.: Madison, WI, 1999.
(81) Farrugia, L. J. *J. Appl. Crystallogr.* **1997**, *30*, 565.
(82) Farrugia, L. J. *J. Appl. Crystallogr.* **1999**, *32*, 837−838.
(83) Arnaud, R.; Juvin, P.; Vallee, Y. *J. Org. Chem.* **1999**, *64*, 8880−8886.
(84) Ruttink, P. J. A.; Burgers, P. C.; Francis, J. T.; Terlouw, J. K. *J. Phys. Chem.* **1996**, *100*, 9694−9697.
(85) Lee, I.; Kim, C. K.; Li, H. G.; Sohn, C. K.; Lee, H. W.; Lee, B. S. *J. Am. Chem. Soc.* **2000**, *122*, 11162−11172.
(86) Typke, V.; Dakkouri, M. *J. Mol. Struct.* **2001**, *599*, 177−193.
(87) Brassington, N. J.; Edwards, H. G. M.; Farwell, D. W.; Long, D. A.; Mansour, H. R. *J. Raman Spectrosc.* **1978**, *7*, 154−157.
(88) Lill, S. O. N.; Rauhut, G.; Anders, E. *Chem.—Eur. J.* **2003**, *9*, 3143−3153.

Electronic Structure of the Sulfonyl and Phosphonyl Functional Groups: NBO/NRT Analysis. NBO analysis provides a powerful means for describing electronic structures in terms that readily translate into the lexicon used by chemists to describe electron density.[89−91] Briefly, NBO analysis involves the optimal transformation of a given *N*-electron wavefunction in terms of a set of *N*/2 localized one-center (corresponding to lone pair) and two-center (corresponding to bonding electron pair) elements. These elements are represented by the highly occupied diagonal entries of the resulting density matrix and provide a molecular description that closely mirrors the Lewis structure depiction. Departures from a strictly localized, Lewis-type structure are represented by nonzero off-diagonal elements of the density matrix, corresponding to antibonding and Rydberg orbitals; occupancy of such orbitals is accompanied by a reduction in the occupancy of the strictly localized orbitals. Thus, the increasing magnitude of off-diagonal elements may be viewed as increasing contributions of the orbitals described by the off-diagonals to the equilibrium structure.

The stabilization afforded by delocalization interactions may be quantitatively estimated by two methods: second-order perturbation analysis and deletion analysis.[92,93] The second-order perturbation analysis approach, employed here, is described in equation (**1**)

$$E(2) = -n_{\text{donor}} \frac{F_{i,j}^{\ 2}}{\Delta E} \qquad (1)$$

where $E(2)$ is the second-order perturbation energy, $F_{i,j}$ corresponds to the matrix element between the orbitals *i* and *j*, $\Delta E = \epsilon_{\text{acceptor}} - \epsilon_{\text{donor}}$, describing the energy difference between the acceptor and donor NBOs, and n_{donor} is the population of the donor orbital.

(89) Weinhold, F. Natural bond orbital methods. In *Encyclopedia of Computational Chemistry*; von Rague Schleyer, P., Ed.; John Wiley and Sons Ltd.: Chichester, U.K., 1998; Vol. 3, pp 1792−1813.

(90) Weinhold, F. *NBO 5.0 Program Manual*; Theoretical Chemistry Institute and Department of Chemistry, University of Wisconsin: Madison, WI, 2001.

(91) Jensen, F. *Introduction to Computational Chemistry*; John Wiley & Sons, Ltd.: Chichester, U.K., 1999; pp 230−232.

(92) During the preparation of this manuscript it was drawn to the authors' attention that caution should be exercised with basis set augmentation using diffuse functions in deletion analysis because of potential effects on the valence space of remote atoms (see Goodman, L.; Sauers, R. R. *J. Comput. Chem.* **2007**, *28*, 269−275). Preliminary tests using several different of the example molecules showed slightly lower occupation of d-orbitals upon removal of diffuse functions from basis sets employed in this study. Despite this, the calculated $E(2)$ values appear relatively independent of whether diffuse functions are employed.

(93) Deletion analysis involves deletion of the off-diagonal element describing the interaction between the relevant orbitals, followed by a single-pass (SCF) energy re-evaluation. The difference between the original and re-evaluated energies, E_{del}, provides an estimate of the stabilization energy afforded to the structure by the relevant orbital interaction. There is general agreement between $E(2)$ and E_{del} values when single orbital interactions are being evaluated. However, when the effects of multiple delocalization interactions are under simultaneous investigation, as they are here, $E(2)$ and E_{del} values may not display adequate agreement. Because of higher-order coupling effects, summation of $E(2)$ values for each individual orbital interaction may not necessarily correspond to an E_{del} value calculated by simultaneous deletion of several interaction elements. Consequently, for the sake of consistency only $E(2)$ values are presented here.

Table 2. Natural Atomic Charges on Selected Sulfonyl and Phosphonyl Species, $(MeOPO_2Y^1)^-$ and $MeOSO_2Y^1$

	$(MeOPO_2Y^1)^-$				$MeOSO_2Y^1$			
Y^1	P	O_{bridge}	$O_{\text{nonbridge}}$	Y1	S	O_{bridge}	$O_{\text{nonbridge}}$	Y^1
OH	+2.75	−0.93	−1.28[a]	−1.06	+2.83	−0.81	−1.01[a]	−0.91
O^-	+2.74	−0.94	−1.35	−1.34	+2.82	−0.83	−1.11	−1.10
NH_2	+2.69	−0.94	−1.27	−1.21	+2.75	−0.83	−1.03	−1.07
NH^-	+2.65	−0.94	−1.34[a]	−1.55	+2.70	−0.85	−1.11[a]	−1.29
CH_3	+2.56	−0.94	−1.28	−0.92	+2.59	−0.83	−1.04	−0.75
CH_2^-	+2.52	−0.95	−1.33	−1.43	+2.53	−0.85	−1.10	−1.14

[a] The nonbridging oxygens in these systems are not symmetrically equivalent; each nonbridging oxygen possesses a slightly different atomic charge [δ(atomic charge) < 0.02]. The values reported are the average of atomic charges on the nonbridging oxygens.

As recently highlighted by Wilke and Weinhold,[67] the Pimentel−Rundle 3-center, 4-electron bonding scheme describes bonding in the hypervalent species Y−X−Z as possessing two resonance contributors: $Y^-\ X^+{-}Z$ and $Y{-}X^+\ Z^-$. This formulation incorporates partial ionic character to describe the bonding within these species and allows description within an s/p-valence framework without the need to invoke octet expansion. Wilke and Weinhold have noted that the 3-center, 4-electron bonding scheme is well described by the NBO framework, with the two resonance contributions $Y^-\ X^+{-}Z$ and $Y{-}X^+\ Z^-$ being described by reciprocal, n→σ* hyperconjugative, donor−acceptor interactions. An $n_Y \rightarrow \sigma^*_{X-Z}$ hyperconjugative interaction, describing donation of electron density from a valence lone pair on Y into the σ*-antibonding orbital of the X−Z bond, results in strengthening of the Y−X bond and a reduction in electron density between atoms X and Z. This $n_Y \rightarrow \sigma^*_{X-Z}$ interaction is therefore representative of the $Y{-}X^+\ Z^-$ resonance form. The reciprocal $n_Z \rightarrow \sigma^*_{X-Y}$ interaction describes the $Y^-\ X^+{-}Z$ resonance form.

The geometries of a series of simple models [$Y^1SO_2Y^2$ and $(Y^1PO_2Y^2)^-$, respectively; Y^1, Y^2= donor and/or acceptor] were optimized without imposing symmetry constraints at the mPW1PW91/6-311++G(3df,2p) level of theory. The electronic structures of these models was then analyzed using natural bond order (NBO) analysis at the RHF/6-311++G-(3df,2p) level of theory. Evidence for the operation of a highly polarized bonding arrangement of the general form $X^+{-}Y^-$ (X = P or S; Y = substituent) in phosphonyl and sulfonyl systems is provided by examination of predicted formal atomic charges. Table 2 shows the formal atomic charges of the methyl phosphate dianion ($MeOPO_3^{2-}$) and the methyl sulfate monoanion ($MeOSO_3^-$). The central atom in both species bears a large formal positive charge, while the substituents on the central atom bear substantial negative charge. The similarity of charge on the central atom in the two structures is striking despite methyl phosphate bearing a formal −2 charge and methyl sulfate bearing a formal −1 charge. Instead, most of the excess negative charge in the methyl phosphate dianion is localized on the nonbridging, "phosphonyl" oxygens. The same relationship is evident upon comparison of the remaining sulfonyl species with the corresponding phosphonyl analogs. In the case of the phosphorus species, our calculations are complementary to

Table 3. Selected NBO Data for Methyl Phosphate and Methyl Sulfate[a]

NBO	occupancy	h_p[b]	%s[b]	%p[b]	%d[b]	polarization toward O (%)
		$MeOSO_3^-$				
$S-O_{bridge}$	1.98	$sp^{4.43}d^{0.24}$	17.6	78.0	4.2	75
$S-O_{nonbridge(anti)}$	1.99	$sp^{2.46}d^{0.11}$	28.0	68.9	3.0	68
$S-O_{nonbridge(syn)}$	1.99	$sp^{2.56}d^{0.11}$	27.2	69.5	3.1	68
$LP(1)-O_{bridge}$	1.97	$sp^{1.13}$	46.9	52.9	0.2	na
$LP(2)-O_{bridge}$	1.95	p	0.0	99.8	0.2	na
$LP(1)-O_{nonbridge(anti)}$	1.98	$sp^{0.41}$	70.7	29.2	0.1	na
$LP(2)-O_{nonbridge(anti)}$	1.87	p	0.0	99.5	0.5	na
$LP(3)-O_{nonbridge(anti)}$	1.84	p	0.0	99.4	0.6	na
$(S-O_{bridge})^*$	0.26	$sp^{4.43}d^{0.24}$	17.6	78.0	4.2	25
$(S-O_{nonbridge(anti)})^*$	0.12	$sp^{2.46}d^{0.11}$	28.0	68.9	3.0	32
$(S-O_{nonbridge(syn)})^*$	0.13	$sp^{2.56}d^{0.11}$	27.2	69.5	3.1	32
		$MeOPO_3^{2-}$				
$P-O_{bridge}$	1.97	$sp^{3.04}d^{0.22}$	17.1	79.0	3.7	85
$P-O_{nonbridge(anti)}$	1.99	$sp^{2.42}d^{0.1}$	28.4	68.6	2.9	77
$P-O_{nonbridge(syn)}$	1.99	$sp^{2.54}d^{0.11}$	27.3	69.5	3.1	77
$LP(1)-O_{bridge}$	1.97	$sp^{1.33}$	42.8	57.0	0.1	na
$LP(2)-O_{bridge}$	1.94	p	0.0	99.9	0.1	na
$LP(1)-O_{nonbridge(anti)}$	1.98	$sp^{0.61}$	62.2	37.7	0.1	na
$LP(2)-O_{nonbridge(anti)}$	1.91	p	0.0	99.6	0.4	na
$LP(3)-O_{nonbridge(anti)}$	1.89	p	0.0	99.6	0.4	na
$(P-O_{bridge})^*$	0.21	$sp^{3.04}d^{0.22}$	17.1	79.0	3.7	15
$(P-O_{nonbridge(anti)})^*$	0.10	$sp^{2.42}d^{0.1}$	28.4	68.6	2.9	23
$(P-O_{nonbridge(syn)})^*$	0.10	$sp^{2.54}d^{0.11}$	27.3	69.5	3.1	23

[a] The number in brackets following the atom designation denotes the specific lone pair participating in the interaction [b] Values are presented for the central atom in bonding and antibonding NBOs and for the relevant atom for lone pair NBOs.

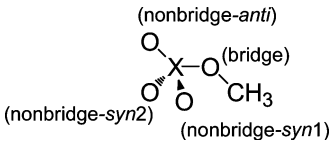

Figure 2. Naming system for methyl phosphate (X = P) and methyl sulfate (X = S). Note that the nonbridging *syn*-oxygens are equivalent by symmetry.

those of Rajca et al.[94] and Horn and Ahlrichs[95] for metaphosphate ion where significant ionicity of bonds resulting in substantial formal charge on P and O were noted.

NBO calculations predict that the valence framework of the sulfonyl and phosphonyl functional groups is highly polarized and suggests the operation of substantial delocalization interactions. In methyl sulfate, bonding between the central atom and its terminal oxygen substituents displays hybridization intermediate between that of an sp^2- and sp^3-hybridized bond (Table 3), with the bonding interactions being highly polarized toward the oxygen substituents (Figure 2). The nonbridging oxygens of methyl sulfate each possess three valence lone pairs. One sp-rich lone pair is essentially localized on oxygen, and does not participate significantly in any delocalization interactions; this is supported by the absence of any significant donor interactions of this lone pair. The two remaining lone pairs on the nonbridging oxygens possess almost exclusive p-character. The occupancy of these p-type orbitals is reduced relative to the sp-rich orbital, presumably through participation of these lone pairs in delocalization interactions.

The precise nature of the delocalization interactions of the terminal oxygen p-type lone pairs is apparent through examination of the second-order perturbation estimates (Table 4). Each nonbridging oxygen participates in three key donor interactions: one involves donation into the antibonding orbital of the central atom-bridging oxygen bond, and the other two interactions involve donation into the antibonding orbitals of the each of the central atom−terminal oxygen bonds. The strongest donor interaction of the terminal oxygens involves donation into the antibonding orbital of the sulfur−bridging oxygen bond. Because each of the terminal oxygens donates strongly into this orbital, this $\sigma^*_{S-O(bridge)}$ orbital represents the principal acceptor for methyl sulfate; the data in Table 3 shows that the population of this acceptor orbital is approximately double the other acceptor orbitals. The two remaining donor interactions involve donation from one nonbridging oxygen into the antibonding orbital of each of the other central atom−nonbridging oxygen bonds. These data establish a reciprocal donor−acceptor interaction between the terminal oxygens, where the oxygen lone pairs act as donors, while simultaneously the central atom−terminal oxygen σ^*-orbital acts as an acceptor. Such reciprocal interactions extend to the bridging oxygen; however, donation from the bridging oxygen is only weak.

Role of d-Orbital Participation in Bonding. The participation of d-orbitals in the bonding of the sulfonyl and phosphonyl functional groups appears, at best, very limited (Table 3). Minor d-character (<5%) is observed for bonding interactions between the central sulfur atom and its substituents in the sulfonyl series; d-orbital character in the phosphorus series is smaller still. The natural atomic orbital (NAO) estimate of the total d-orbital occupancy of the central sulfur atom of methyl sulfate amounts to 0.2e, indicating only relatively minor d-orbital participation. Furthermore, the calculated atomic charges described above, with significant positive charge on the central sulfur or phosphorus, are inconsistent with significant d-orbital participation, which should be associated with an increase in electron density at the central atom.

An alternative method of investigating d-orbital participation in bonding is to study the effects of d-orbital exclusion from basis sets on the optimized geometry. Structures of methyl sulfate and methyl phosphate optimized at the mPW1PW91/6-311++G level of theory possessed longer predicted bonds between the central atom and its oxygen substituents relative to geometry optimizations performed at the mPW1PW91/6-311++G(3df,2p) level of theory (Table 5). Second-order perturbation analysis on these structures indicates that exclusion of d-orbitals in the basis set used for geometry optimization also results in a relative reduction in the estimated strength of delocalization interactions; a decrease in the strength of these interactions is associated with increased bond lengths. Consequently, the observed bond elongation may be an artifact of loss of delocalization interactions within the s/p framework caused by the loss of the polarization function capacity of d-orbital inclusion, rather than by loss of d-orbital occupancy.

(94) Rajca, A.; Rice, J. E.; Streitweiser, A., Jr.; Schaefer, H. F., III. *J. Am. Chem. Soc.* **1987**, *109*, 4189−4192.
(95) Horn, H.; Ahlrichs, R. *J. Am. Chem. Soc.* **1990**, *112*, 2121−2124.

Table 4. *E*(2) Values for Major Donor−Acceptor Interactions in Methyl Phosphate and Methyl Sulfate

		$MeOSO_3^-$ (X = S)			$MeOPO_3^{2-}$ (X = P)		
donor orbital[a]	acceptor orbital (X = central atom)	*E*(2) (kcal mol^{-1})	Δ*E* (au)	$F_{i,j}$	*E*(2) (kcal mol^{-1})	Δ*E* (au)	$F_{i,j}$
$n_{O(bridge)(1)}$	$\sigma^*_{X-O(nonbridge-anti)}$	2.2	1.53	0.053	1.6	1.53	0.045
$n_{O\ (bridge)(2)}$	$\sigma^*_{X-O(nonbridge-syn1)}$	5.9	1.17	0.076	4.5	1.19	0.066
$n_{O\ (bridge)(2)}$	$\sigma^*_{X-O(nonbridge-syn2)}$	5.7	1.17	0.074	4.5	1.19	0.066
$n_{O(nonbridge-anti)(2)}$	$\sigma^*_{X-O(nonbridge-syn1)}$	22.2	1.07	0.138	17.7	1.08	0.124
$n_{O(nonbridge-anti)(2)}$	$\sigma^*_{X-O(nonbridge-syn2)}$	22.1	1.07	0.138	17.7	1.08	0.124
$n_{O(nonbridge-anti)(3)}$	$\sigma^*_{X-O(bridge)}$	36.0	0.78	0.153	29.4	0.84	0.143
$n_{O(nonbridge-syn1)(2)}$	$\sigma^*_{X-O(nonbridge-anti)}$	18.4	1.09	0.126	14.7	1.1	0.113
$n_{O(nonbridge-syn1)(2)}$	$\sigma^*_{X-O(nonbridge-syn2)}$	23.7	1.08	0.143	19.1	1.09	0.129
$n_{O(nonbridge-syn1)(3)}$	$\sigma^*_{X-O(bridge)}$	38.1	0.78	0.158	30.7	0.84	0.147
$n_{O(nonbridge-syn2)(2)}$	$\sigma^*_{X-O(nonbridge-anti)}$	18.3	1.09	0.126	14.7	1.1	0.113
$n_{O(nonbridge-syn2)(2)}$	$\sigma^*_{X-O(nonbridge-syn1)}$	23.7	1.08	0.143	19.1	1.09	0.129
$n_{O(nonbridge-syn2)(3)}$	$\sigma^*_{X-O(bridge)}$	38.2	0.78	0.158	30.7	0.84	0.147

[a] See Figure 2 for nomenclature details.

Table 5. Comparison of Selected Predicted Bond Lengths Optimized with and without Inclusion of d-Orbitals

	mPW1PW91/ 6-311++G(3df,2p)	mPW1PW91/ 6-311++G
	$MeOSO_3^-$	
$S-O_{bridge}$ (Å)	1.651	1.866
$S-O_{nonbridge(anti)}$ (Å)	1.440	1.616
$S-O_{nonbridge(syn)}$ (Å)	1.449	1.628
	$MeOPO_3^{2-}$	
$P-O_{bridge}$ (Å)	1.743	1.873
$P-O_{nonbridge(anti)}$ (Å)	1.512	1.619
$P-O_{nonbridge(syn)}$ (Å)	1.521	1.632

Further evidence against significant d-orbital participation is provided by natural resonance theory (NRT) analysis. NRT analysis provides a means for the description of the total electron density of a given system in terms of a series of idealized resonance forms.[71−73] Each resonance form is given a weighting, reflecting its relative contribution to the total electron density. For methyl sulfate, the major resonance contributor identified by NRT was the "polar" valence electron depiction, where a single bond connects each of the substituents to the central sulfur, with three lone pairs localized on each of the terminal, nonbridging oxygens (Chart 1). Resonance forms involving "double-bond, no-bond" interactions between the terminal oxygens contribute substantially to the overall electronic structure as do double-bond, no-bond resonance forms arising from donation by the terminal oxygens into the antibonding orbital of the central atom−bridging oxygen bond. The weightings apportioned to the two different double-bond, no-bond resonance forms in methyl sulfate supports significant delocalization interactions this species. Notably, contributions from structures where the central sulfur possessed formal hypervalency were not given any weighting in the analysis.

Summary of NBO/NRT Analysis of Bonding in Sulfonyl and Phosphonyl Systems. The results of NRT analysis provide insight into the relative contributions of polarized X^+-Y^--type interactions and $n_Y \rightarrow \sigma^*_{X-Y}$ hyperconjugative interactions to bonding in sulfonyl and phosphonyl species. Identification of the polar resonance structure as the reference structure in both of these species suggests bonding is predominately of the form X^+-Y^-; however, the weightings given to various "double-bond, no-bond" resonance forms indicate hyperconjugation plays a significant role in bonding in methyl phosphate and methyl sulfate. If bonding in methyl sulfate and methyl phosphate was solely an *m*-center, *n*-electron arrangement, the weighting of the double-bond, no-bond resonance forms should be greater, possibly to the point where the double-bond, no-bond resonance forms would represent reference structures. Further evidence against a pure *m*-center, *n*-electron bonding arrangement is the predicted occupancy of the lone pairs participating in this interaction (Table 3), which are higher than would be expected for fully delocalized lone pairs.

Taken together, the NBO and NRT descriptions of the bonding arrangement in sulfonyl and phosphonyl systems suggest that they share a common bonding framework composed of highly polarized interactions between the central atom and its substituents of the form X^+-Y^-. These interactions are augmented by a highly delocalized 5-center, 8-electron bonding network composed of reciprocal $n_Y \rightarrow \sigma_{X-Y^*}$ hyperconjugative interactions. This bonding arrangement is composed of multiple 3-center, 4-electron-type interactions, each of which operates between an oxygen atom, the central sulfur or phosphorus atom, and any other substituent. The proposed bonding model extends the relatively simple bonding model of previous studies,[44,53,61,63−66,68] involving operation of individual $n_Y \rightarrow \sigma^*_{X-Y}$ hyperconjugative interactions, and does not require d-orbital participation to rationalize bonding in sulfonyl and phosphonyl systems. Finally, it should be noted that *m*-center, *n*-electron bonding without recourse to valence expansion beyond eight electrons at sulfur been proposed in hypervalent sulfur diimide and triimide species.[30]

Differences between Bonding in the Sulfonyl and Phosphonyl Functional Groups. The eye-catching biological and chemical similarities between sulfonyl and phosphonyl groups encouraged us to compare their electronic structures in more detail. The phosphonyl systems participate in donor−acceptor interactions to a substantially smaller degree than their sulfur analogs, as evidenced by reduced *E*(2) values, reduced occupancy of the relevant antibonding orbitals, and increased localization of donor lone pairs on

Chart 1. NRT Summary of Methyl Sulfate and Methyl Phosphate [RHF/6-311++G(3df,2p)]

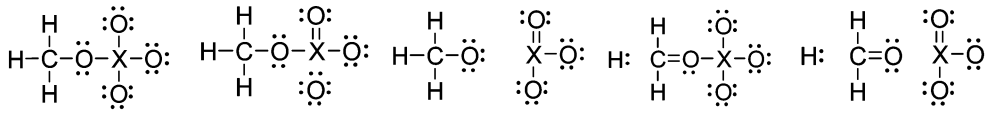

	reference structure				
$MeOSO_3^-$ (X = S) % weighting	59.2%	22.0%[a]	14.1%[a]	4.7%[a]	0.0%
$MeOPO_3^{2-}$ (X = P) % weighting	67.6%	16.7%[a]	11.1%[a]	3.7%[a]	1.0%

[a] The percentage value quoted is the sum of all resonance contributors of this general formulation.

oxygen (Tables 3 and 4). Furthermore, the valence bonding interactions between oxygen and phosphorus are substantially more polarized toward oxygen than the equivalent bonds in the sulfonyl systems (Table 3). Such differences in bonding most likely have their origin in the larger electronegativity difference between phosphorus and oxygen (Δ(EN) = 1.4), compared to that between sulfur and oxygen (Δ(EN) = 1.0).

Comparison of selected second-order perturbation parameters provides insight into reduced donor−acceptor interactions in the phosphonyl systems relative to the sulfonyl systems (Table 4). The strength of hyperconjugative interactions is influenced by the difference in energy between the participating orbitals and their relative spatial orientation. For strong interaction, the energy difference between the participating orbitals should be minimal (reflected in a small ΔE value in second-order perturbation analysis), while spatial overlap of the two orbitals should be maximized (reflected in a large $F_{i,j}$ value). The acceptor interactions of the phosphonyl nonbridging oxygen bonds display essentially the same ΔE value as the corresponding interactions in the sulfonyl system; however, the orbital overlap element $F_{i,j}$ is reduced in every case. Because the predicted bond lengths in methyl phosphate are longer than the corresponding bond lengths in methyl sulfate (Table 5), this suggests that the relative reduction in $F_{i,j}$ arises because participating orbitals cannot overlap as efficiently because of increased spatial separation. This increased spatial separation probably arises as a consequence of increased electrostatic repulsion between the nonbridging oxygens in phosphate, relative to sulfate. The ΔE value in sulfonyl or phosphonyl systems is essentially the same for these interactions, but the energy of both the donor and acceptor orbitals in methyl phosphate are increased relative to the corresponding orbitals in methyl sulfate. In contrast to the central atom−nonbridging oxygen bonds, the acceptor interactions of the bridging atom−oxygen bond show both an increase in ΔE and a decrease in $F_{i,j}$, indicating that both energetic and spatial factors are responsible for the reduced interaction in the phosphonyl system relative to the sulfonyl system. These data suggest a more polarized bonding arrangement with greater ionic or closed-shell interaction in the phosphonyl systems and with shared donor−acceptor interactions making a smaller contribution to the equilibrium electronic structure than for the corresponding sulfonyl analogs.

The bonding model proposed here is consistent with complementary studies using either an atoms-in-molecules (AIM) or electron localization function (ELF) approach. Chesnut and Quin, using an AIM approach, have proposed an essentially identical bonding scheme for sulfonyl systems to that presented here, where "backbonding" interactions (corresponding to donor−acceptor interactions) contribute a significant proportion (some 40%) of S−O bond order.[96] Similarly, the differences in phosphoryl and sulfuryl bonding are evident in an AIM and ELF study performed by Boily on bonding in XO_4 anions (X = Si, P, S, Cl, Ge, As, Se, Br).[97] Boily proposed that, with few exceptions, the X−O bonding interaction in XO_4 anions is intermediate between a shared (covalent) interaction and closed-shell (ionic) interaction, with greater closed-shell character correlated to an increasing electronegativity difference between X and O. This trend is consistent with that observed here, where bonding interactions in the phosphonyl systems are more polarized toward oxygen and participate to a lesser extent in donor−acceptor interactions, relative to the sulfonyl system.

Trends in Donor−Acceptor Interactions and Implications for the Electronic and Geometric Structures of the Sulfonyl and Phosphonyl Moieties. We next sought to investigate the effect of substituent variation upon the electronic structure of the sulfonyl and phosphonyl groups. Substituent variation should result in changes in both the nature of the polar interactions and the donor−acceptor interactions. However, because the hyperconjugative com-

(96) Chesnut, D. B.; Quin, L. D. *J. Comput. Chem.* **2004**, *25*, 734−738.
(97) Boily, J. F. *J. Phys. Chem. A* **2002**, *106*, 4718−4724.

Table 6. S−Y^1 Bond Polarization within $MeOSO_2Y^1$ (Y^1 = OH, NH_2, CH_3, O^-, NH^-, CH_2^-)

	% polarization toward Y^1 in Y^1−X	
Y^1	neutral form	conjugate base
OH	71.3	67.9
NH_2	64.4	59.8
CH_3	52.3	49.6

ponent of bonding is a delocalized form of bonding, it is reasonable to anticipate that it will be more susceptible to remote substituent effects than the polarized component of bonding. To test the relative effects of substituent variation on the polar versus the hyperconjugative component of bonding, the effect of deprotonation of the model series $MeOSO_2Y^1$ (Y^1 = OH, NH_2, CH_3) was examined. Deprotonation results in increased charge localization on Y^1, which is anticipated to cause opposing electronic effects within the polar and hyperconjugative frameworks. Increased charge localization on Y^1 should cause an increase in bond polarization if polar effects dominate, resulting from an increase in the closed shell or ionic nature of the bonding interaction. However, if hyperconjugative effects dominate, a decrease in bond polarization is expected because of increased donation of the extra electron density into the hyperconjugative framework. Examination of the bond polarization between S and Y^1 (Table 6) shows that in each case deprotonation is associated with a decrease in S−Y^1 bond polarization, consistent with a relatively greater change within the donor−acceptor framework than in localized, polar interaction. Table 7 presents the sum of $E(2)$ donor and acceptor estimates for several sulfonyl and phosphonyl systems. These systems possess substituents that vary in their donor and σ^*-acceptor ability, allowing investigation of changes to the global electronic structure of the sulfonyl and phosphonyl groups caused by substituent variation.

Trends in Predicted σ^*-Acceptor Ability. Predicted $\sigma^*_{S-Y^2}$ and $\sigma^*_{P-Y^2}$ acceptor ability in $Y^1SO_2Y^2$ and $(Y^1PO_2Y^2)^-$ increases with alteration of the identity of Y^2 from left to right across the first row (Y^2 = CH_3, NH_2, OH, F; Table 7). This increase parallels the increasing electronegativity of Y^2, and increasing X−Y^2 bond polarity (consistent with an increase in the polarization coefficient of the antibonding orbital on the central atom). For instance, in the $(SO_3Y^2)^-$ series, the predicted $\sigma^*_{S-Y^2}$ acceptor ability is Y^2= CH_3 ($\sum E(2)$ = 73.5 kcal mol^{-1}) < NH_2 ($\sum E(2)$ = 93.6 kcal mol^{-1}) < OH ($\sum E(2)$ = 113.3 kcal mol^{-1}) < F ($\sum E(2)$ = 139 kcal mol^{-1}), and in the $(PO_3Y^2)^{2-}$ series, the predicted $\sigma^*_{P-Y^2}$ acceptor ability is Y^2 = CH_3 ($\sum E(2)$ = 66.5 kcal mol^{-1}) < NH_2 ($\sum E(2)$ = 78.9 kcal mol^{-1}) < OH ($\sum E(2)$ = 87.8 kcal mol^{-1}). In the $(SO_3Y^2)^-$ series, enhanced σ^*-acceptor ability arises as a result of a modest decrease in the ΔE term coupled with a more dramatic increase in the $F_{i,j}$ term, while in the $(PO_3Y^2)^{2-}$ series, enhanced interactions arise exclusively from changes to the $F_{i,j}$ term (Table 8). Our findings are consistent with those of Alabugin and Zeidan in their systematic study of the σ^*-acceptor ability of C−Y bonds in acyclic substituted ethanes, where the predicted σ^*_{C-Y} acceptor ability increased across a period.[98] Alabugin and Zeidan observed that σ^*_{C-Y}-orbitals display polarization inverse to that of their corresponding σ-bonding orbitals. Consequently, increased C−Y bond polarization, arising from a greater electronegativity difference between C and Y, is associated with an increased σ^*_{C-Y}-orbital coefficient on C, facilitating more facile $n_{Y^1} \rightarrow \sigma^*_{C-Y^2}$ overlap; this enhanced interaction is ultimately reflected in increased $F_{i,j}$ values.

In the same study, Alabugin and Zeidan investigated σ^*-acceptor ability within a group and found that predicted σ^*_{C-Y}-acceptor ability increased down a group, despite a decrease in the electronegativity of Y. These workers observed that, while the matrix overlap element $F_{i,j}$ was roughly proportional to electronegativity for all the studied species, ΔE was the term critical in determining the relative acceptor ability within a group. For all the phosphorus systems, the observed trend in acceptor ability is $\sigma^*_{P-F} < \sigma^*_{P-Cl} < \sigma^*_{P-Br}$, consistent with the trend observed by Alabugin and Zeidan. The same trend is also observed in the predicted σ^*_{S-Hal} acceptor ability for the $(SO_3Y^2)^-$ series. In both cases, the relative σ^*_{P-Hal}- or σ^*_{S-Hal}-acceptor ability is determined by the ΔE term and not the $F_{i,j}$ term (Table 9).

In the $NH_2SO_2Y^2$ and $CH_3SO_2Y^2$ series, the relative σ^*_{S-Hal} acceptor ability remains consistent with the series described above for bromine and chlorine, but the σ^*_{S-F} acceptor ability displays anomalous behavior (Table 7). In the $NH_2SO_2Y^2$ series, the relative σ^*_{S-Hal} acceptor ability is similar for the three halogens ($d\sum E(2) \approx 7$ kcal mol^{-1}); consequently, small changes in either the $F_{i,j}$ or the ΔE terms alters the relative ordering of σ^*_{S-Hal}-acceptor ability. In this series, the unfavorable increase in ΔE associated with an increase in electronegativity between Br and F is compensated for by a relatively larger favorable increase in $F_{i,j}$, resulting in slightly stronger σ^*_{S-Hal}-acceptor ability for fluorine relative to either bromine or chlorine (Table 9). In the $CH_3SO_2Y^2$ series, the predicted σ^*_{S-F} acceptor ability orbital is exceedingly poor because of the high estimated energy of this orbital [$E(\sigma^*_{S-F}) = 0.73$ au; cf., $E(\sigma^*_{S-Br}) = 0.06$ au and $E(\sigma^*_{S-Cl}) = 0.11$ au]. Taken with the data from the $(SO_3Y^2)^-$ and $(PO_3Y^2)^{2-}$ series, this suggests that the σ^*-acceptor orbital energies within the sulfonyl series are more susceptible to substituent effects than in the phosphonyl systems, especially with respect to sulfur−fluorine interactions.

Implications of Increased Acceptor Ability on Structure and Reactivity. The presence of a strong σ^*-acceptor within the systems under investigation results in enhanced donor−acceptor hyperconjugative interactions. Figure 3 shows a plot of the sum of the predicted σ^*-acceptor interactions of Y^2 and the total predicted n_O-donor interactions of the nonbridging oxygens (Y^2 = halogen, CH_3, NH_2, OH). This plot shows a strong correlation between these parameters and suggests that improvements in acceptor ability result in

(98) Alabugin, I. V.; Zeidan, T. A. *J. Am. Chem. Soc.* **2002**, *124*, 3175−3185.

Table 7. Sum of Selected Donor−Acceptor Interactions [$\sum E(2)$] for Substituents in $Y^1SO_2Y^2$ and $(Y^1PO_2Y^2)^-$ (All Values in kcal mol^{-1})[a]

$(SO_3Y^2)^-$							$CH_3SO_2Y^2$						
	$Y^1 = O^-$		Y^2		$O_{nonbridge}$ (av)			$Y^1 = NH_3$		Y^2		$O_{nonbridge}$ (av)	
Y^2	donor	acceptor	donor	acceptor	donor	acceptor	Y^2	donor	acceptor	donor	acceptor	donor	acceptor
F	101.3	60.6	17.4	139.5	101.4	60.9	F	9.0	48.1	41.1	0.6	51.7	52.4
Cl	107.8	58.6	7.3	154.7	107.9	58.9	Cl	8.8	54.2	13.9	107.9	112.4	42.8
Br	112.2	57.8	5.1	168.7	112.3	57.7	Br	9.2	52.6	10.2	110.7	113.2	41.3
CH_3	81.5	58.6	4.8	73.5	81.5	58.6	OH	6.7	42.7	17.8	68.9	78.7	35.2
NH_2	87.1	62.2	12.0	93.6	87.6	59.2	H	6.8	53.0	na	69.5	94.7	36.8
OH	93.7	59.2	16.8	113.3	92.9	61.9							
H	84.5	56.4	nd	84.7	84.7	56.4							

$(PO_3Y^2)^{2-}$[b]							$(CH_3PO_2Y^2)^-$						
	$Y^1 = O^-$		Y^2		$O_{nonbridge}$ (av)			$Y^1 = NH_3$		Y^2		$O_{nonbridge}$ (av)	
Y^2	donor	acceptor	donor	acceptor	donor	acceptor	Y^2	donor	acceptor	donor	acceptor	donor	acceptor
CH_3	67.9	46.5	2.3	66.5	67.9	46.5	F	4.3	54.1	21.9	80.7	90.8	36.5
NH_2	70.4	49.3	8.0	78.9	71.7	46.8	Cl	6.0	51.1	11.1	92.7	97.4	34.0
OH[d]	74.2	46.9	13.6	87.8	72.8	49.3	Br	6.7	49.3	7.7	103.4	101.6	32.5
H	69.1	44.6	na	73.4	69.1	44.6	OH	4.3	51.9	19.0	72.6	87.6	37.0
							H	3.9	49.9	na	59.4	82.1	29.5

$NH_2SO_2Y^2$[c]							$(MeOPO_2Y^1)^-$						
	$Y^1 = NH_2$		Y^2		$O_{nonbridge}$ (av)			Y^1		$Y^2 = OMe$		$O_{nonbridge}$ (av)	
Y^2	donor	acceptor	donor	acceptor	donor	acceptor	Y^1	donor	acceptor	donor	acceptor	donor	acceptor
F	27.9	73.5	24.3	121.4	117.3	45.9	CH_3	4.5	52.5	19.2	73.4	88.8	37.7
Cl	28.9	72.3	15.3	114.5	116.0	44.8	CH_2^-	32.6	37.6	10.7	91.1	77.9	35.1
Br	29.5	70.5	11.4	116.0	116.2	43.3	NH_2	15.2	62.1	19.7	78.1	91.4	38.8
CH_3	21.0	72.4	7.0	63.1	96.5	42.7	NH^-	44.6	43.0	11.4	94.4	77.6	
OH	23.6	70.0	22.1	100.3	109.8	47.5						(76.0)	(35.7)
H	23.2	68.0	na	73.8	99.7	40.4	OH	23.3	70.0	21.5	76.7	94.1	40.7
												(90.9)[e]	(42.4)[e]
							O^-	75.7	45.6	12.2	90.7	74.7	50.5

$(NH_2PO_2Y^2)^-$							$MeOSO_2Y^1$						
	$Y^1 = NH_2$		Y^2		$O_{nonbridge}$ (av)			Y^1		$Y^2 = OMe$		$O_{nonbridge}$ (av)	
Y^2	donor	acceptor	donor	acceptor	donor	acceptor	Y^1	donor	acceptor	donor	acceptor	donor	acceptor
F	16.9	64.4	23.3	87.6	93.1	37.3	CH_3	7.4	56.5	23.0	86.4	102.6	46.4
Cl	20.3	61.1	10.4	100.0	99.1	34.4	CH_2^-	64.1	37.9	11.7	126.7	89.3	44.9
Br	22.2	55.3	7.9	111.1	102.8	32.8	NH_2	22.4	66.8	20.8	95.9	108.1	48.3
CH_3	13.5	61.9	4.0	56.7	83.4	32.9	NH^-	78.1	48.8	13.8	121.5	92.7	48.3
OH[d]	15.4	61.0	19.1	78.3	90.4	38.0						(91.1)	(57.1)
H	14.0	62.2	na	59.0	84.9	31.3	OH	27.2	87.1	26.9	92.8	115.0	49.6
												(112.6)	(52.2)
							O^-	93.5	56.8	15.8	113.4	93.2	62.7

[a] The NBO default cutoff of 0.5 kcal mol^{-1} was employed in these calculations. [b] The halogen analogs were unable to be optimized for this analysis because of the unimolecular decomposition of these species during attempts at their geometry optimization. [c] This data represents one conformer about the N−S or N−P bond; the other conformer, in which the nitrogen lone pair is *syn* to the substituents on the central atom, possesses lower n_N-donor ability because of poorer overlap with the antibonding orbital of the X−Y bond. [d] The optimized geometries of this series possess a single imaginary frequency related to X−OH rotation; however, for the sake of comparative purposes, this structure was chosen as the reference structure. [e] The nonbridging oxygens in these species showed asymmetry with respect to donor and acceptor ability because of the asymmetry of the Y^1 substituent; consequently, values for both nonbridging oxygens are presented.

Table 8. Selected $E(2)$ Parameters for $(SO_3Y^2)^-$ and $(PO_3Y^2)^{2-}$

		$(SO_3Y^2)^-$			$(PO_3Y^2)^{2-}$		
		acceptor orbital $\sigma^*_{S-Y^2}$			acceptor orbital $\sigma^*_{P-Y^2}$		
donor orbital	Y^2	$E(2)$ (kcal mol^{-1})	ΔE (au)	$F_{i,j}$	$E(2)$ (kcal mol^{-1})	ΔE (au)	$F_{i,j}$
$n_{O(nonbridge-anti)(3)}$	CH_3	23.8	0.81	0.125	22.2	0.83	0.123
$n_{O(nonbridge-anti)(3)}$	NH_2	32.3	0.80	0.146	26.7	0.84	0.136
$n_{O(nonbridge-anti)(3)}$	OH	36.7	0.77	0.154	28.9	0.84	0.142

greater contributions of hyperconjugation to bonding. Enhanced hyperconjugative interactions are manifested as changes in their geometric and electronic structures, including a decrease in the formal charge on the sulfonyl and phosphonyl nonbridging oxygens, a decrease in the X−O (X = P or S) bond length, and a contraction of the Y^2−X−O bond angle (Table 10). The structural changes described above are consistent with those encountered with movement along a reaction coordinate involving unimolecular decomposition of these species; attempts to optimize the geometry of the PO_{3-Hal} species, which are expected to exhibit strong hyperconjugative donor−acceptor interactions, resulted in unimolecular elimination of the halogen to generate monomeric metaphosphate. Additionally, unimolecular elimination was also observed when attempting to optimize the geometry of the conjugate base species of trifluoromethyl mesylate and trifluoromethyl sulfamate. These results suggest that the degree of participation in donor−acceptor interac-

Table 9. Selected $E(2)$ Values for Y^2 = Hal

	$Y^1SO_2Y^2$ donor orbital = $n_{O(nonbridge-syn1)(3)}$			$(Y^1PO_2Y^2)^-$ donor orbital = $nO_{(nonbridge-syn1)(3)}$		
Y^2	$E(2)$ (kcal mol^{-1})	ΔE (au)	$F_{i,j}$	$E(2)$ (kcal mol^{-1})	ΔE (au)	$F_{i,j}$
			$Y^1 = O^-$			
F	46.5	0.71	0.169	nd[a]	nd[a]	nd[a]
Cl	51.5	0.53	0.155	nd[a]	nd[a]	nd[a]
Br	56.3	0.48	0.155	nd[a]	nd[a]	nd[a]
			$Y^1 = NH_2$			
F	50.2	0.75	0.177	37.9	0.83	0.161
Cl	43.4	0.59	0.146	42.9	0.64	0.151
Br	44.4	0.54	0.141	47.6	0.58	0.153
			$Y^1 = CH_3$			
F	<0.5	nd[b]	nd[b]	39.6	0.83	0.164
Cl	51.0	0.58	0.156	45.2	0.63	0.154
Br	52.1	0.53	0.151	50.3	0.58	0.156

[a] The phosphorus series was unable to be optimized for this analysis because of the unimolecular decomposition of these species during attempts at their geometry optimization. [b] The $E(2)$ value for this interaction was below the default cutoff of 0.5 kcal mol^{-1}.

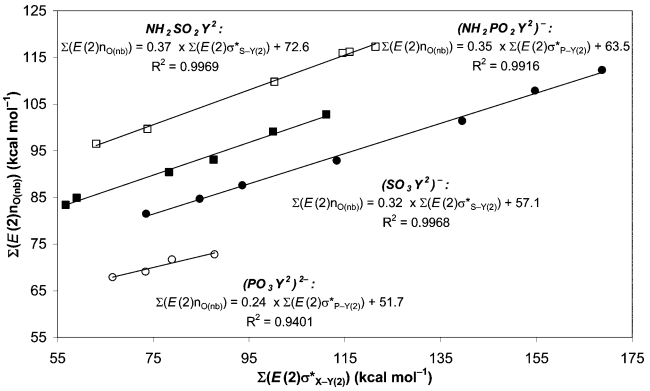

Figure 3. Plot of the sum of the acceptor ability of Y^2 and the sum of the donor ability of the sulfonyl or phosphonyl nonbridging oxygens. Data are from the $NH_2SO_2Y^2$ (□), $(NH_2PO_2Y^2)^-$ (■), $(SO_3Y^2)^-$ (●), and $(PO_3Y^2)^{2-}$ (○) series; Y^2 = halogen, CH_3, NH_2, OH.

Table 10. Selected Geometric Parameters for $(SO_3Y^2)^-$ and $(PO_3Y^2)^{2-}$

Y^2	$\Sigma E(2)$ (acceptor) (kcal mol^{-1})	$O_{(nonbridge-anti)}$ atomic charge	$X-O_{(nonbridge-anti)}$ bond length (Å)	$O_{(nonbridge-anti)}-X-Y^2$ angle (deg)
		$(SO_3Y^2)^-$, X = S		
F	139.5	−1.08	1.439	102.1
Cl	154.7	−1.06	1.438	101.7
Br	168.7	−1.05	1.438	101.4
CH_3	73.5	−1.13	1.457	104.4
NH_2	93.6	−1.11	1.449	102.9
OH	113.3	−1.11	1.449	101.7
H	84.7	−1.12	1.453	103.7
		$(PO_3Y^2)^{2-}$, X = P		
CH_3	66.5	−1.36	1.527	103.3
NH_2	78.9	−1.35	1.522	102.7
OH	87.8	−1.34	1.516	101.6
H	73.4	−1.36	1.527	103.2

tions is important in determining the ease of unimolecular decomposition for sulfonyl and phosphonyl groups.

Trends in Predicted Donor Ability. Examination of trends in the predicted donor ability of a substituent Y^1 is complicated by multiple potential donor orbitals on Y^1. The lone pairs on Y^1 and Y^1-H σ-bond electron pairs may both act as donors, and to fully understand donor substituent effects, it is therefore necessary to examine trends in both the predicted donor ability of individual orbitals on Y^1 and in the sum of donor interactions for the entire substituent Y^1. Table 11 lists selected $E(2)$ values for the $MeOSO_2Y^1$ and $(MeOPO_2Y^1)^-$ (Y^1 = CH_3, CH_2^-, NH_2, NH^-, OH, O^-). Examination of donor ability of individual orbitals within these systems suggests that trends in predicted donor ability generally parallel that expected from consideration of electronegativity and charge density.

Table 11. Selected Individual Donor Interactions for $MeOSO_2Y^1$ and $(MeOPO_2Y^1)^-$

		$MeOSO_2Y^1$ acceptor orbital: $\sigma^*_{S-O(bridge)}$			$(MeOPO_2Y_1)^-$ acceptor orbital: $\sigma^*_{P-O(bridge)}$		
Y^1	donor orbital	$E(2)$ (kcal mol^{-1})	ΔE (au)	$F_{i,j}$	$E(2)$ (kcal mol^{-1})	ΔE (au)	$F_{i,j}$
CH_3	$\sigma_{C-H(anti)}$	2.2	1.12	0.047	1.4	1.2	0.037
CH_2^-	$n_{C(1)}$	47.4	0.55	0.147	23.8	0.68	0.117
NH_2	$n_{N(1)}$	13.2	0.90	0.101	9.2	0.99	0.089
NH^-	$n_{N(2)}$	43.0	0.64	0.151	31.0	0.72	0.137
OH	$n_{O(nonbridge-anti)(2)}$	12.2	0.97	0.101	11.0	1.03	0.098
O^-	$n_{O(nonbridge-anti)(3)}$	36.0	0.78	0.153	29.4	0.84	0.143

Comparison of methyl mesylate ($MeOSO_2CH_3$) and its phosphorus analog ($MeOPO_2CH_3^-$) reveals that the donor ability of a lone pair greatly exceeds that of an Y^1-H σ-bond [$E(2)$ $n_C \rightarrow \sigma^*_{S-OCH_3}$ = 47.4 kcal mol^{-1}, cf., $E(2)$ $\sigma_{C-H} \rightarrow \sigma^*_{S-OCH_3}$ = 2.2 kcal mol^{-1}; $E(2)$ $n_C \rightarrow \sigma^*_{P-OCH_3}$ = 23.8 kcal mol^{-1}, cf., $E(2)$ $\sigma_{C-H} \rightarrow \sigma^*_{P-OCH_3}$ = 1.4 kcal mol^{-1}] (Table 11). In addition to conversion of a comparatively poor donor to a strong donor, deprotonation of the neutral species Y^1H_Z (Y^1 = C, N, O; Z = 1−3) to generate the singly charged $(Y^1H_{Z-1})^-$ anion also results in an increase in the predicted donor ability of the other orbitals on Y^1 through favorable energetic and geometric changes. Deprotonation causes greater charge localization on Y^1, resulting in destabilization of all donor orbitals on Y^1 and promoting stronger donation through improved energetic overlap between donor and acceptor orbitals; this is reflected in a favorable decrease in the ΔE term. Moreover, deprotonation is accompanied by a reduction in the predicted $X-Y^1$ (X = P or S) bond length. The reduced atomic separation between the central atom and Y^1 in the conjugate base series facilitates more efficient overlap between the participating orbitals and is reflected in a favorable increase in the $F_{i,j}$ element.

Alkylation of Y, like protonation, also causes a reduction in substituent donor ability. Comparison of $E(2)$ values for the nonbridging oxygens in $(SO_3OH)^-$ [$\sum E(2)_{donor}$ = 93.7 kcal mol^{-1}] with the bridging oxygen of its alkylated analog, $MeOSO_2OH$ [$\sum E(2)_{donor}$ = 26.9 kcal mol^{-1}] reveals a significant decrease in donor ability accompanying alkylation. The effect of alkylation is highlighted within methyl sulfate ($MeOSO_3^-$): the predicted n_O-donor ability of the bridging methoxide oxygen is significantly exceeded by the nonbridging oxygens [$\sum E(2)_{donor(MeO)}$ = 15.8 kcal mol^{-1} and $\sum E(2)_{donor(O^-)}$ = 93.2 kcal mol^{-1}].

The differences in donor ability of substituent orbitals were investigated next. Unfortunately, this comparison cannot be achieved with the corresponding neutral series because of the absence of a lone pair on the neutral methyl substituent. The most relevant series for comparison across the periodic table is the isoelectronic conjugate base series $(MeOSO_2Y^1)^-$

Table 12. Selected Geometric Parameters for $MeOSO_2Y^1$ and $(MeOPO_2Y^1)^-$

Y^1	$\sum E(2)$ donor (kcal mol^{-1})	X−Y^1 bond length (Å)	bond polarization (% at Y^1)	X−O_{bridge} bond length (Å)	bond polarization (% at O_{bridge})	X− $O_{nonbridge(syn)}$ bond length (Å)[a]	$O_{nonbridge(syn)}$ atomic charge
				$MeOSO_2Y^1$ X = S			
OH	27.2	1.568	71	1.574	72	1.414	−1.01
						(1.422)	
O^-	93.5	1.440	68	1.651	75	1.449	−1.11
NH_2	22.4	1.616	64	1.592	72	1.421	−1.02
NH^-	78.1	1.529	60	1.672	74	1.446	−1.11
						(1.456)	
CH_3	7.4	1.756	52	1.589	72	1.427	−1.04
CH_2^-	64.1	1.626	50	1.697	75	1.450	−1.10
				$(MeOPO_2Y^1)^-$ X = P			
OH	23.3	1.633	81	1.651	82	1.479	−1.28
						(1.488)	
O^-	75.7	1.512	77	1.743	86	1.521	−1.35
NH_2	15.2	1.689	76	1.656	82	1.484	−1.27
NH^-	44.6	1.617	71	1.754	85	1.513	−1.34
						(1.523)	
CH_3	4.5	1.821	68	1.663	82	1.489	−1.28
CH_2^-	32.6	1.740	62	1.758	84	1.512	−1.33

[a] The nonbridging oxygens in these species showed asymmetry with respect to donor and acceptor ability because of the asymmetry of the Y^1 substituent; consequently, values for both nonbridging oxygens are presented.

and $(MeOPO_2Y^1)^{2-}$ (Y^1 = CH_2, NH, O; Table 11). For the sulfonyl conjugate base series, the n_{Y^1}-donor ability decreases with the increasing electronegativity of Y^1 [$E(2)_{nC\rightarrow\sigma^*S-OCH_3}$ = 47.4 kcal mol^{-1} > $E(2)_{nN\rightarrow\sigma^*S-OCH_3}$ = 43.0 kcal mol^{-1} > $E(2)_{nO\rightarrow\sigma^*S-OCH_3}$ = 36.0 kcal mol^{-1}]. The differences in the predicted donor ability in this series arises almost exclusively as a result of changes to the ΔE term, reflecting the increase in charge stabilization on Y^1 with increasing electronegativity; the $F_{i,j}$ term is essentially invariant. In the phosphonyl series, the predicted donor ability displays the same general trend in the ΔE term with decreasing electronegativity but also displays a pronounced decrease in the $F_{i,j}$ element. By analogy with the differences in $F_{i,j}$ values between methyl phosphate and methyl sulfate (discussed above), the relatively greater changes in the $F_{i,j}$ values probably reflect a greater contribution from electrostatic repulsion of negatively charged terminal substituents in the phosphonyl systems because of the greater formal negative charges within the phosphonyl systems, resulting in poorer orbital overlap between terminal substituents and the central phosphorus atom.

The total predicted donor ability of a substituent Y^1 is determined by the formal charge on the substituent and the nature of the donor orbitals on Y^1. Introduction of a formal negative charge onto the substituent Y^1 strongly enhances the total donor ability. Indeed, the sum of the total donor interactions in the weakest anionic species in the $MeOSO_2Y^1$ series substantially exceeds the total donor interactions of the strongest neutral species [$\sum E(2)$ = 27.2 kcal mol^{-1}, cf., $\sum E(2)$ = 64.1 kcal mol^{-1} for $MeOSO_3H$ and for $MeOSO_2CH_2^-$, respectively; Table 7].

Within each of the neutral and anionic series, the nature of donor orbitals on Y^1 determines the relative order of total donor ability of Y^1. Each substituent under investigation here possesses three donor orbitals that donate into either the σ^*-orbital of the central atom−bridging oxygen (X−O_{bridge}) bond or the σ^*-orbitals of the central atom−nonbridging oxygen bonds (X−$O_{nonbridge}$). As a lone pair represents a more potent donor orbital than an Y^1−H σ-bond, more lone pairs on Y^1 increases the total donor ability of Y^1. The total substituent donor ability for both the neutral and anionic series is thus O > N > C; this order is the reverse of the strength of the donor ability of the individual orbitals on Y^1.

Structural Implications of Increased Donor Ability. As for alterations in σ^*-acceptor ability, changes in donor ability of individual orbitals are associated with geometric and electronic changes consistent with enhanced donor/acceptor hyperconjugation. Pairwise comparison of each neutral species with its conjugate base shows enhanced hyperconjugation is associated with a shorter bond between the donor substituent and the central atom concomitant with a longer, more-polarized bonding arrangement between the central atom and the acceptor substituent, consistent with greater σ^*-character in the interaction between the central atom and the acceptor (Table 12).

Introduction of a strong donor orbital into a sulfonyl or phosphonyl group causes additional, subtle alterations to the global electronic structure of these systems, particularly with respect to the central atom−nonbridging oxygen (X−$O_{nonbridge}$) bonds. While the nonbridging oxygens represent potent donor orbitals, the central atom−nonbridging oxygen bonds are excellent σ^*-acceptors, resulting in favorable reciprocal hyperconjugative interactions. The σ^*-acceptor role of X−$O_{nonbridge}$ bonds becomes particularly important when another strong donor orbital is present. The presence of a substituent with strong donor orbitals in these systems causes a significant increase in the predicted σ^*-acceptor role of the X−$O_{nonbridge}$ bond. This is manifested in a slightly longer predicted X−$O_{nonbridge}$ bond length and a larger predicted negative charge localized on the nonbridging oxygen (Table 12). In tandem with an increase in the predicted σ^*-acceptor role of the X−$O_{nonbridge}$ bond is a small decrease in the donor ability of the nonbridging oxygens. The structural and electronic manifestations of increased donation oppose those occurring with increased σ^*-acceptor ability; consequently, an increase in σ^*-character of a bond renders donation by orbitals on the nonbridging oxygens

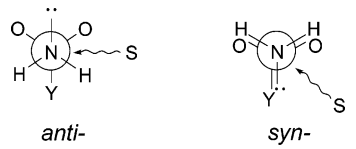

Figure 4. *anti*- (allowing for maximal $n_N \rightarrow \sigma^*_{S-Y^2}$ overlap) and *syn*-conformers about the N−S bond of sulfonamides and sulfamates.

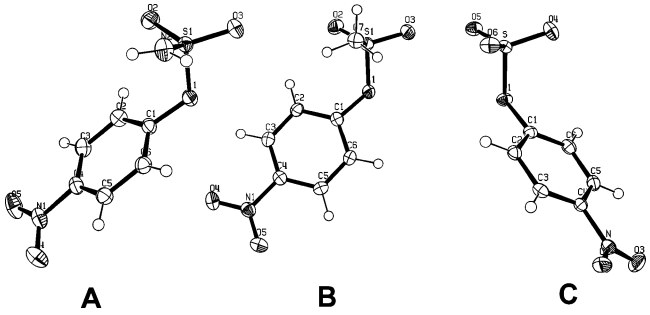

Figure 5. ORTEP diagram of single crystal, low-temperature X-ray structures of 4-nitrophenylsulfamate (A), potassium 4-nitrophenylmesylate (B), and potassium 4-nitrophenylsulfate monoester (C). Note the potassium has been removed from C for the sake of clarity. Thermal ellipsoids are at 50% probability.

more difficult. The plasticity of the $X-O_{nonbridge}$ bond highlights the reciprocal donor−acceptor nature of bonding in these systems, where the relative degree to which substituents act as donors or acceptors is dependent upon the nature of other substituents within the system.

An important consequence of the bonding scheme proposed for the sulfonyl and phosphonyl functional groups is that the relative substituent donor−acceptor ability should influence the equilibrium conformation of sulfonyl- and phosphonyl-containing species. In most experimentally determined X-ray structures of such species, the observed conformer with respect to rotation about the substituent-central atom bond is that which maximizes spatial overlap between the most potent donor orbital on the substituent with the most effective acceptor orbital in the sulfonyl or phosphonyl system. This conformation is more common with increasing donor or σ^*-acceptor ability. For instance, in the solid-state crystal structures of aryl and alkyl sulfamates discussed below, the only conformation seen about the sulfur−nitrogen bond is that where the predicted position of the nitrogen lone pair is *anti*-periplanar to the sulfur-bridging oxygen bond, allowing for maximum $n_{Y(1)} \rightarrow \sigma^*_{S-OR}$ overlap (Figures 4 and 5). This line of reasoning does not imply that maximization of favorable orbital overlap interactions is the sole factor in the determination of conformational equilibria of sulfonyl and phosphonyl containing compounds: there are numerous reported experimentally determined structures of sulfonyl and phosphonyl containing species that display features inconsistent with delocalization interactions being the sole determinant of the dominant equilibrium conformation. A survey of sulfonamide structures in Cambridge Structural Database performed by Ohwada and co-workers[99] revealed that both the *syn*- and *anti*-isomers with respect to the N−S bond are represented in the reported structures of sulfonamides. In the case of the *syn*-isomer, where the amine protons eclipse the sulfonyl oxygens, favorable $n_N \rightarrow \sigma^*_{S-Y(2)}$ overlap is not maximized. Furthermore, in a recently reported gas-phase electron-diffraction study of benzenesulfonamide ($C_6H_5SO_2NH_2$),[100] the eclipsed *syn*-conformation about the S−N bond is favored over the *anti*-conformation. This conformational preference was tentatively ascribed to a stabilizing electrostatic interaction between the sulfonyl oxygens and the amine protons; it may equally reflect that the dominant donor in this system is the phenyl group.

Crystallographic Evidence for Reciprocal Hypervalent Bonding. While considerable amounts of structural data has been gathered for phosphonyl systems, there is a shortfall of the corresponding data for sulfonyl systems. To provide experimental evidence for operation of the bonding arrangement in sulfonyl systems predicted by the above calculations, structure−reactivity correlations were constructed using single-crystal low-temperature X-ray data for three series of alkyl and aryl sulfate, sulfamate, and mesylate esters. Altering electron demand at the sulfonyl center will directly affect the electronic structure at the site of substitution in ways that should manifest as systematic changes in molecular geometry. Such changes represent an important test for any bonding model of the sulfonyl functional group. It should be noted that there is no absolute experimental measure of bond length and determinations by X-ray crystallography suffer from random errors arising from the local environment within the crystal, as well as potentially from systematic error arising from libration. The latter can be minimized through determination at low temperature and random errors can be minimized by consideration of trends in bond length within related series rather than exact values. Additionally, ionic compounds such as sulfate monoesters may have variations arising from different counterions, and therefore, all structures reported herein contained identical counterions. Although this reduces the potential for errors, the geometry of the counterion with respect to the sulfate monoester anion, and differences in crystal packing may still result in nonsystematic variations between even apparently closely related structures, and so some caution is advised in drawing conclusions from such data.

The effect of altering electron density at the sulfonyl center was examined through comparison of structural parameters between the three series. In line with the n_Y-donor ability of the donor atoms predicted from the above calculations, the sulfate monoesters ($Y^1 = O^-$) should possess the greatest donor ability, the sulfamate esters ($Y^1 = NH_2$) an intermediate ability, and the mesylate esters (mesylates, $Y^1 = CH_3$) the poorest donor ability. Consequently, structural changes associated with increased electron density in the donor−acceptor component of bonding are expected to be most pronounced for the sulfate monoesters.

The effect of electron withdrawal on molecular geometry at the sulfonyl center was studied through construction of a

(99) Ohwada, T.; Okamoto, I.; Shudo, K.; Yamaguchi, K. *Tetrahedron Lett.* **1998**, *39*, 7877−7880.

(100) Petrov, V.; Petrova, V.; Girichev, G. V.; Oberhammer, H.; Giricheva, N. I.; Ivanov, S. *J. Org. Chem.* **2006**, *71*, 2952−2956.

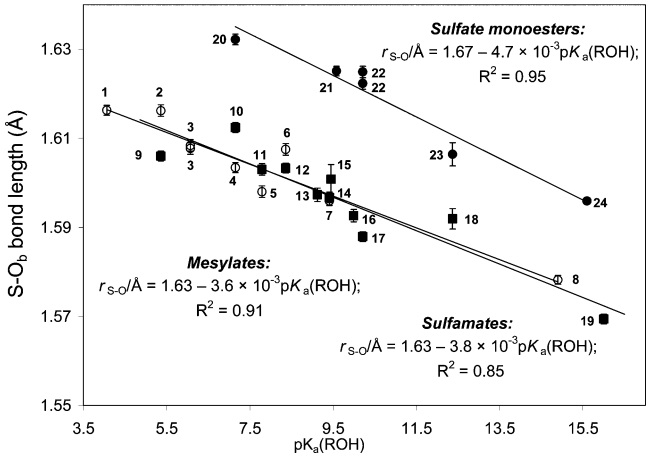

Figure 6. Structure−reactivity plot of $r_{S-O(bridge)}$ vs pK_a (ROH) for sulfate monoesters (●), sulfamates (■), and mesylates (○). Compounds are mesylates (**1**−**8**) (**1**) 2,4-dinitrophenyl mesylate, (**2**) 3,4-dinitrophenyl mesylate, (**3**) 4-nitro-3-(trifluoromethyl)phenyl mesylate (2 independent molecules in unit cell), (**4**) 4-nitrophenyl mesylate, (**5**) 4-cyanophenyl mesylate, (**6**) 3-nitrophenyl mesylate, (**7**) 4-chlorophenyl mesylate, and (**8**) 4-nitrobenzyl mesylate, sulfamates (**9**−**19**) (**9**) 3,4-dinitrophenylsulfamate ester, (**10**) 4-nitrophenylsulfamate ester, (**11**) 4-cyanophenylsulfamate ester, (**12**) 3-nitrophenylsulfamate ester, (**13**) 3-chlorophenylsulfamate ester, (**14**) 4-chlorophenylsulfamate ester, (**15**) 4-iodophenylsulfamate ester, (**16**) phenylsulfamate ester, (**17**) 4-methoxyphenylsulfamate esters, (**18**) 2,2,2-trifluoroethylsulfamate ester, (**19**) ethylsulfamate ester, and sulfate monoesters (**20**−**25**) (**20**) potassium 4-nitrophenylsulfate, (**21**) potassium 4-acetamidophenylsulfate, (**22**) potassium 4-methoxyphenylsulfate (2 independent molecules in unit cell), (**23**) potassium 2,2,2-trifluoroethylsulfate, (**24**) potassium methyl sulfate. Crystallographic details for the sulfate monoester and sulfamate ester series have been reported previously.[37] Errors denote estimated standard deviation of bond lengths.

Brønsted plot of selected structural parameters versus the pK_a values of the parent alcohol. Examination of the dependence of sulfur−bridging oxygen (S−O_{bridge}) bond length upon the pK_a value of the parent alcohol *within* each of the mesylate, sulfamate, and sulfate series (Figure 6) reveals that the S−O_{bridge} bond length displays an inverse correlation to the pK_a value of the parent alcohol, with S−O_{bridge} bonds becoming progressively longer with decreasing pK_a value. The magnitude and sign of the slope of this Brønsted plot is consistent with those obtained for phosphate monoesters by Jones and Kirby using X-ray crystallography (slope = -8×10^{-3} Å/(pK_a unit))[101] and by Cheng et al. using vibrational spectroscopy in aqueous solution (slope = -2.57×10^{-3} Å/(pK_a unit)).[102] Consequently, increased electron withdrawal at the bridging oxygen of sulfonyl and phosphonyl systems is associated with structural changes consistent with an enhanced donor/acceptor interaction with the σ^*_{S-O}- and σ^*_{P-O}-orbitals. Enhancement of the hyperconjugative interaction is expected to arise from stabilization of the acceptor orbitals, rather than increased donation from the donor orbitals on the nonbridging atoms.

Notably, the results above differ from those of Sorensen-Stowell and Hengge, where ^{31}P NMR spectroscopy of ^{18}O isotope shifts was used to assess changes to P−O_{bridge} bond order for phosphate monoesters in aqueous[103] and nonaqueous[104] solvents. Neither study found any evidence for changes in bond order with changes to leaving group pK_a value. Collectively, the solid and solution-phase data suggest that, at least for phosphate monoesters, changes to bond length with substituent variation in the solid state are less pronounced (or even absent) in the solution phase. This may be a result of differences in the electrostatic microenvironments of the solid and liquid phases or from conformational mobility that is possible in solution but not the solid phase. In this regard it is worthwhile noting that all X-ray structures used in the study of Jones and Kirby possessed a staggered conformation about the P−O_{bridge} bond, ensuring maximal n → σ^* interactions.[101] While such a conformation is also expected to be preferred in the solution phase, time-averaged contributions from transient high-energy eclipsed conformations may reduce the magnitude of the effect of n → σ^* interactions on bond length. Thus it should be noted that the structural effects described for substituent variation in the solid phase may not apply to the same degree in the solution phase.

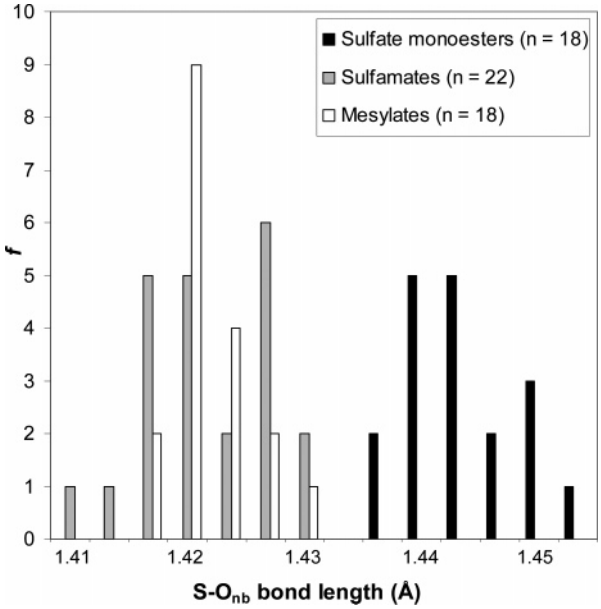

Figure 7. Histogram of S−$O_{nonbridge}$ bond lengths in sulfate monoesters, sulfamates, and mesylates.

Evidence for the operation of reciprocal hyperconjugative interactions within the sulfonyl group was obtained through examination of changes in the "sulfonyl", sulfur−nonbridging oxygen bond (S−$O_{nonbridge}$) parameters caused by altering electron demand at the sulfonyl center. Introduction of substituents with increased donor ability, which should result in increased occupancy of the S−$O_{nonbridge}$ antibonding orbital, is associated with S−$O_{nonbridge}$ bond elongation (Figure 7). The S−$O_{nonbridge}$ bond lengths of the sulfate monoester series [mean(S−$O_{nonbridge}$)$_{sulfate}$ = 1.4450(12) Å, n = 18] are longer than those of the sulfamate ester series,

(101) Jones, P. G.; Kirby, A. J. *J. Am. Chem. Soc.* **1984**, *106*, 6207−6212.
(102) Cheng, H.; Nikolic-Hughes, I.; Wang, J. H.; Deng, H.; O'Brien, P. J.; Wu, L.; Zhang, Z. Y.; Herschlag, D.; Callender, R. *J. Am. Chem. Soc.* **2002**, *124*, 11295−11306.
(103) Sorensen-Stowell, K.; Hengge, A. C. *J. Org. Chem.* **2005**, *70*, 4805−4809.
(104) Sorensen-Stowell, K.; Hengge, A. C. *J. Org. Chem.* **2005**, *70*, 8303−8308.

[mean($S-O_{nonbridge}$)$_{sulfamate}$ = 1.4231(11) Å, n = 22] or the mesylate ester series [mean($S-O_{nonbridge}$)$_{mesylate}$ = 1.4233(8) Å, n = 18].

The X-ray crystal structures reveal longer $S-O_{nonbridge}$ bond lengths in the sulfate monoester series relative to the sulfamate and mesylate ester series (Figure 6). This interesting data can be explained by considering the relative donor−acceptor relationship between the sulfonyl oxygens and the donor substituent Y^1 within the mesylate ($Y^1 = CH_3$), sulfamate ($Y^1 = NH_2$), and sulfate ester ($Y^1 = O^-$) series. Each of the three nonbridging oxygens in sulfate monoesters possesses approximately the same n_Y-donor ability, which is much greater than either the sulfamate amino group or the mesylate methyl group. Consequently, each of the sulfonyl oxygen bonds have increased σ^*_{S-O} character and reduced n_Y-donation from the sulfonyl oxygens, which manifests as increased bond lengths. In systems where the sulfonyl oxygens represent the most potent n_Y-donor substituents, for example, in both the mesylate and sulfamate ester series, the n_Y-donor ability of the sulfonyl oxygens is expected to make a major contribution to the $S-O_{nonbridge}$ bonding interaction leading to shortened $S-O_{nonbridge}$ bond lengths compared to the sulfate ester series.

The similarity in the $S-O_{nonbridge}$ bond lengths displayed by the mesylates and sulfamates implies the sulfonyl oxygens are the major n_Y-donor in these systems and obscure the effects of the differences between the NH_2 and CH_3 groups (Figure 6). This is supported by the calculated donor ability of these substituents; the total donor ability of the substituent O^- and the strength of its individual $n \rightarrow \sigma^*$ donor components significantly exceed those of the mesylate methyl substituent or the sulfamate amino substituent. Alternatively, the lack of difference in these structural parameters of the sulfamate and mesylate esters may result from the greater n_Y-donor ability of the amino group over a CH_3 group, cancelling out the greater acceptor ability of the $\sigma^*_{S-NH_2}$-orbital relative to that of the $\sigma^*_{S-CH_3}$-orbital.

The disparity in the pK_a values over which each of the three series range potentially complicates analysis of the relationship between $S-O_{nonbridge}$ bond length and the donor ability of Y^1 if the $S-O_{nonbridge}$ bond length is dependent on the pK_a value. However, the pK_a value of the parent alcohol does not appear to appreciably influence $S-O_{nonbridge}$ bond length. Examination of the relationship between $S-O_{nonbridge}$ bond length and pK_a values (See Figure S1, Supporting Information) reveals a small and only poorly correlated dependence. Furthermore, the $S-O_{nonbridge}$ bond lengths in representatives from each series that share a common parent phenol, 4-nitrophenylsulfate monoester [$r_{s-o(nonbridge)}$ = 1.4412(13), 1.4409(12), 1.4373(13) Å], 4-nitrophenylsulfamate [$r_{s-o(nonbridge)}$ = 1.4267(11), 1.4192(11) Å], and 4-nitrophenylmesylate [$r_{s-o(nonbridge)}$ = 1.4201(12), 1.4229(12) Å] are consistent with the relationship described above. These results imply that our analysis of the relationship between donor ability of Y^1 and $S-O_{nonbridge}$ bond length is not influenced by the differences in the range of pK_a values in the three series.

The differences in $S-O_{bridge}$ bond lengths *between* each of the three sulfonyl series likely result from differences in the n_Y-donor ability of the terminal substituents. Examination of Figure 6 reveals that the $S-O_{bridge}$ bond lengths in sulfate monoesters are longer than those of either the sulfamate or the mesylate series. The sulfate monoester series possesses only oxygen terminal substituents, which are much stronger donors than the terminal substituents of either the mesylate ($2 \times O + CH_3$) or the sulfamate ($2 \times O + NH_2$); consequently, donation into the $\sigma^*_{S-O(bridge)}$-orbital is expected to be more effective for sulfate monoesters, and this is reflected in the X-ray crystal structures as longer $S-O_{bridge}$ bonds.

We have previously reported a structure correlation examining the dependence of the sum of the $O_{nonbridge}-S-O_{nonbridge}$ bond angles with the $S-O_{bridge}$ bond length for the sulfate monoester series.[37] An increase in the sum of the nonbridging angles was correlated to an increase in $S-O_{bridge}$ bond length [$\sum(O_{nonbridge}-S-O_{nonbridge}$ angles) = 49.3(r_{S-O}/Å) + 262°), R^2 = 0.86], reflecting a trend from a distorted tetrahedral arrangement [$\sum(O_{nonbridge}-S-O_{nonbridge}$ angles) = 328.5° in an ideal tetrahedron] toward a trigonal planar arrangement of the nonbridging substituents [$\sum(O_{nonbridge}-S-O_{nonbridge}$ angles) = 360° for SO_3] with increasing $S-O_{bridge}$ bond length. These data were interpreted to provide insight into the structural manifestations occurring with movement along a reaction coordinate of unimolecular elimination of sulfur trioxide from sulfate monoesters.[37] However, these data also provide evidence for strengthened $n_O \rightarrow \sigma^*_{S-O(bridge)}$ donation by *each* of the nonbridging oxygens in the ground state. With increasing acceptor ability of the $S-O_{bridge}$ antibonding orbital, stronger n_O-donation from each of the nonbridging oxygens will result in increased "double-bond" character of the $S-O_{nonbridge}$ interactions and greater sp^2 character at sulfur; this is seen in the more "sulfur trioxide-like" geometry observed about the central sulfur as $S-O_{bridge}$ bond length increases.

Last, Jones and Kirby have reported structure−reactivity correlations for phosphate monoesters and triesters with changing pK_a value of the parent alcohol.[101] Substituent alkylation will result in removal of formal charge and should substantially reduce n_Y-donor ability. Thus, phosphate monoester dianions, which possess much more potent donor substituents than the corresponding neutral triesters, should exhibit a greater sensitivity to increasing σ^*_{P-O} acceptor ability than the triesters. This is reflected in Jones and Kirby's structural data where the slope of the Brønsted plot of $P-O_{bridge}$ bond length for phosphate monoesters was nearly twice that of the corresponding triesters.[101]

An alternative explanation for the observed trends in structural parameters can be made by invoking a purely electrostatic argument that considers Lewis representations where the central atom conforms to the octet rule and integral positive and negative charges are located on the central atom and peripheral substituents, respectively. According to this approach, the observed differences in structural parameters between the three series and within each series arise simply through differences in the electrostatic repulsion between the

negatively charged terminal substituents. For example, the longer $S-O_{nonbridge}$ bonds in the sulfate monoester series relative to the sulfamate or mesylate series arise because of the greater charge localized on the terminal substituents of the sulfate monoesters. This causes greater through-space electrostatic repulsion between the three terminal substituents and a subsequent increase in their interatomic distances. Likewise, the effect of substituent variation on $S-O_{bridge}$ bond length can be explained by a decrease in the electron density on the bridging oxygen caused by increasing electron demand from the substituent. This electrostatic argument is consistent with the proposed bonding model because it assumes a large degree of charge localization on the terminal substituents, implying a charge separated, highly polarized mode of bonding between the terminal substituents and the central sulfur or phosphorus atom. These assumptions are borne out by the calculated atomic charges and electronic structure predicted by NBO analysis. Indeed, it is very probable that the observed trends in structural parameters in the three sulfonyl systems seen here and in the previously published structure−reactivity correlation of phosphate esters[101] arise because of contributions from both changes in the donor−acceptor framework and electrostatic interactions.

Conclusions

Despite the burgeoning weight of computational evidence against d-orbital participation in sulfonyl and phosphonyl systems, introductory textbooks still explain bonding in these groups, and sulfate in particular, using octet violation about the central sulfur and phosphorus atoms. In this study we provide computational and experimental evidence against this Lewis representation, with a particular focus on sulfonyl groups. Investigation of the hybridization of the central sulfur and phosphorus atoms in sulfonyl and phosphonyl systems, and formal charges throughout such systems by NBO analysis, provided little support for significant d-orbital participation in any of these species. These results are supported by NRT deconvolution of the electronic structures of methyl sulfate and methyl phosphate ions into their resonance contributors, which showed no contribution from octet violating resonance forms. NBO analyses of the electronic structures of sulfonyl and phosphonyl groups predict that they are highly polarized with significant contributions from reciprocal hyperconjugation, where substituents off the central sulfur or phosphorus act simultaneously as donors and acceptors. X-ray crystallographic data for three series of sulfate monoester, sulfamate esters and mesylate esters give rise to systematic trends in bond lengths and geometries with substituent variation. Together, the computational and experimental data support a bonding network in sulfonyl and phosphonyl groups comprised of highly polarized interactions between the central phosphorus and sulfur atoms and their substituents with significant contributions from reciprocal hyperconjugative interactions of the form $n \rightarrow \sigma^*$. Our study provides computational evidence supported by experimental evidence for a simple, alternative Lewis depiction with octet conformity that is readily applied and should be easily accepted even at an introductory level.

Acknowledgment. This work was supported by the Australian Research Council (DP0449625). Support of the Victorian Institute for Chemical Sciences High Performance Computing Facility is gratefully acknowledged. Profs Carl H. Schiesser, Leo Radom, and Lionel Goodman are gratefully acknowledged for their generous assistance with calculations. Goh Yit Wooi is gratefully acknowledged for her assistance with X-ray crystallography. E.D. is supported by the Sir John and Lady Higgins Scholarship.

Supporting Information Available: Structure−reactivity correlation plot of pK_a(ROH) vs $S-O_{nonbridge}$ bond length, synthesis, characterization data and crystallization conditions for mesylates **1**−**8**, crystallization conditions and X-ray crystallographic data for mesylates **1**−**8**, optimized parameters in Cartesian coordinates (standard orientation) for all species studied by computational means, crystallization information files for mesylates **1**−**8**. This material is available free of charge via the Internet at http://pubs.acs.org.

IC700687T